

1 **Quantifying Soil Carbon Accumulation in Alaskan Terrestrial Ecosystems during the Last**
2 **15,000 Years**

3

4

5 Sirui Wang¹, Qianlai Zhuang^{1,2*}, Zicheng Yu³

6 ¹Department of Earth, Atmospheric, and Planetary Sciences, Purdue University, West Lafayette,
7 Indiana, 47907

8 ²Department of Agronomy, Purdue University, West Lafayette, IN 47907

9 ³Department of Earth and Environmental Sciences, Lehigh University, Bethlehem, PA 18015

10 Correspondence to: qzhuang@purdue.edu

11

12

13

14

15

16

17

18

19

20

21

22

23

24

25

26

27

28 **Abstract:** Northern high latitudes contain large amounts of soil organic carbon (SOC), in which
29 Alaskan terrestrial ecosystems account for a substantial proportion. In this study, the SOC
30 accumulation in Alaskan terrestrial ecosystems over the last 15,000 years was simulated using a
31 process-based biogeochemistry model for both peatland and non-peatland ecosystems.
32 Comparable with the previous estimates of 25-70 Pg C in peatland and 13-22 Pg C in non-
33 peatland soils within 1-m depth in Alaska using peat core data, our model estimated a total SOC
34 of 36-63 Pg C at present, including 27-48 Pg C in peatland soils and 9-15 Pg C in non-peatland
35 soils. Current vegetation stored 2.5-3.7 Pg C in Alaska with 0.3-0.6 Pg C in peatlands and 2.2-
36 3.1 Pg C in non-peatlands. The simulated average rate of peat C accumulation was 2.3 Tg C yr⁻¹
37 with a peak value of 5.1 Tg C yr⁻¹ during the Holocene Thermal Maximum (HTM) in the early
38 Holocene, four folds higher than the average rate of 1.4 Tg C yr⁻¹ over the rest of the Holocene.
39 The SOC accumulation slowed down, or even ceased, during the neoglacial climate cooling after
40 the mid-Holocene, but increased again in the 20th century. The model-estimated peat depths
41 ranged from 1.1 to 2.7 m, similar to the field-based estimate of 2.29 m for the region. We found
42 that the changes in vegetation and their distributions were the main factors to determine the
43 spatial variations of SOC accumulation during different time periods. Warmer summer
44 temperature and stronger radiation seasonality, along with higher precipitation in the HTM and
45 the 20th century might have resulted in the extensive peatland expansion and carbon
46 accumulation.

47 **Keywords:** Carbon, Peatlands, Alaska, Modelling, Climate

48

49

50

51 **1. Introduction**

52 Global surface air temperature has been increasing since the middle of the 19th century
53 (Jones and Mogberg, 2003; Manabe and Wetherald, 1980, 1986). Since 1970, the warming trend
54 has accelerated at a rate of 0.35 °C per decade in northern high latitudes (Euskirchen et al., 2007;
55 McGuire et al., 2009). It is predicted that the warming will continue in the next 100 years (Arctic
56 Climate Impact Assessment 2005; Intergovernmental Panel on Climate Change (IPCC), 2013,
57 2014). The land surface in northern high latitudes (>45° N) occupies 22% of the global surface
58 and stores over 40% of the global soil organic carbon (SOC) (McGuire et al., 1995; Melillo et al.,
59 1995; McGuire and Hobbie, 1997). Specifically, the northern high latitudes were estimated to
60 store 200-600 Pg C (1 Pg C = 10¹⁵ g C) in peatland soils depending on the depth considered
61 (Gorham, 1990, 1991; Yu, 2012), 750 Pg C in non-peatland soils (within 3 m) (Schuur et al.,
62 2008; Tarnocai et al., 2009; Hugelius et al., 2014), and additional 400 Pg C in frozen loess
63 deposits of Siberia (Zimov et al., 2006a). Peatland area is around 40 million hectares in Alaska
64 compared with total 350 million hectares in northern high latitudes (Kivinen and Pakarinen,
65 1981). Alaskan peatlands account for the most peatland area in the USA and cover at least 8% of
66 the total land area (Bridgham et al., 2006). To date, the regional soil C and its responses to the
67 climate change are still with large uncertainties (McGuire et al., 2009; Loisel et al., 2014).

68 The warming climate could increase C input to soils as litters through stimulating plant
69 net primary productivity (NPP) (Loisel et al., 2012). However, it can also decrease the SOC by
70 increasing soil respiration (Yu et al., 2009). Warming can also draw down the water table in
71 peatlands by increasing evapotranspiration, resulting in higher decomposition as the aerobic

72 respiration has a higher rate than anaerobic respiration in general (Hobbie et al., 2000). SOC
73 accumulates where the rate of soil C input is higher than decomposition. The variation of climate
74 may switch the role of soils between a C sink and a C source (Davidson and Janssens, 2006;
75 Davidson et al., 2000; Jobbagy and Jackson, 2000). Unfortunately, due to the data gaps of field-
76 measurement and uncertainties in estimating regional C stock (Yu, 2012), with limited
77 understanding of both peatlands and non-peatlands and their responses to climate change, there is
78 no consensus on the sink and source activities of these ecosystems (Frolking et al., 2011; Belyea,
79 2009; McGuire et al., 2009).

80 Both observation and model simulation studies have been applied to understand the long-
81 term peat C accumulation in northern high latitudes. Most field estimations are based on series of
82 peat-core samples (Turunen et al., 2002; Roulet et al., 2007; Yu et al., 2009; Tarnocai et al.,
83 2009). However, those core analyses may not be adequate for estimating the regional C
84 accumulation due to their limited spatial coverage. To date, a number of model simulations have
85 also been carried out. For instance, Frolking et al. (2010) developed a peatland model
86 considering the effects of plant community, hydrological dynamics and peat properties on SOC
87 accumulation. The simulated results were compared with peat-core data. They further analyzed
88 the contributions of different plant functional types (PFTs) to the peat C accumulation. However,
89 this 1-D model has not been evaluated with respect to soil moisture, water-table depth, methane
90 fluxes, and carbon and nitrogen fluxes and has not been used in large spatial-scale simulations by
91 considering other environmental factors (e.g., temperature, vapor pressure, and radiation). In
92 contrast, Spahni et al. (2013) used a dynamic global vegetation and land surface process model
93 (LPX), based on LPJ (Sitch et al., 2003), imbedded with a peatland module, which considered
94 the nitrogen feedback on plant productivity (Xu-Ri and Prentice, 2008) and plant biogeography,

95 to simulate the SOC accumulation rates of northern peatlands. However, climatic effects on SOC
96 were not fully explained, presumably due to its inadequate representation of ecosystem processes
97 (Stocker et al., 2011, 2014; Kleinen et al., 2012). The Terrestrial Ecosystem Model (TEM) has
98 been applied to study C and nitrogen dynamics in the Arctic (Zhuang et al., 2001, 2002, 2003,
99 2015; He et al., 2014). However, the model has not been calibrated and evaluated with peat-core
100 C data, and has not been applied to investigate the regional peatland C dynamics. Building upon
101 these efforts, recently we fully evaluated the peatland version of TEM (P-TEM) including
102 modules of hydrology (HM), soil thermal (STM), C and nitrogen dynamics (CNDM) for both
103 upland and peatland ecosystems (Wang et al., 2016).

104 Here we used the peatland-core data for various peatland ecosystems to parameterize and
105 test P-TEM (Figure 1). The model was then used to quantify soil C accumulation of both
106 peatland and non-peatland ecosystems across the Alaskan landscape since the last deglaciation.
107 This study is among the first to examine the peatlands and non-peatlands C dynamics and their
108 distributions and peat depths using core data at regional scales.

109

110 **2. Methods**

111 **2.1. Overview**

112 To conduct regional simulations of carbon accumulation for both uplands and peatlands,
113 we first parameterized the P-TEM for representative ecosystems in Alaska. Second, we
114 organized the regional vegetation and peatland distribution data, spatial basal age data for all
115 peatland grid cells based on site-level soil core data, and climate data for each period during the
116 Holocene. Finally, we conducted the regional simulations and sensitivity analysis.

117 2.2 Model Description

118 In P-TEM (Wang et al., 2016), peatland soil organic C (SOC) accumulation is determined
119 by the difference between NPP and aerobic and anaerobic decomposition. Peatlands accumulate
120 C where NPP is greater than decomposition, resulting in positive net ecosystem production
121 (NEP):

$$122 \quad NEP = NPP - R_H - R_{CH_4} - R_{CWM} - R_{CM} - R_{COM} \quad (1)$$

123 P-TEM was developed based on the Terrestrial Ecosystem Model (TEM) at a monthly
124 step (Zhuang et al., 2003; 2015). It explicitly considers the process of aerobic decomposition (R_H)
125 related to the variability of water-table depth; net methane emission after methane oxidation
126 (R_{CH_4}); CO₂ emission due to methane oxidation (R_{CWM}) (Zhuang et al., 2015); CO₂ release
127 accompanied with the methanogenesis (R_{CM}) (Tang et al., 2010; Conrad, 1999); and CO₂ release
128 from other anaerobic processes (R_{COM} , e.g., fermentation, terminal electron acceptor (TEA)
129 reduction) (Keller and Bridgham, 2007; Keller and Takagi, 2013). For upland soils, we only
130 considered the heterotrophic respiration under aerobic condition (Raich, 1991). For detailed model
131 description see Wang et al. (2016).

132 We modeled peatland soils as a two-layer system for hydrological module (HM) while
133 keeping the three-layer system for upland soils (Zhuang et al., 2002). The soil layers above the
134 lowest water table position are divided into: (1) moss (or litter) organic layer (0-10 cm); and (2)
135 humic organic layer (10-30 cm) (Wang et al., 2016). Based on the total amount of water content
136 within those two unsaturated layers, the actual water table depth (WTD) is estimated. The water
137 content at each 1 cm above the water table can be then determined after solving the water
138 balance equations (Zhuang et al., 2004).

139 In the STM module, the soil vertical profile is divided into four layers: (1) snowpack in
140 winter, (2) moss (or litter) organic layer, (3) upper and (4) lower humic organic soil (Wang et al.,
141 2016). Each of these soil layers is characterized with a distinct soil thermal conductivity and heat
142 capacity. We used the observed water content to drive the STM (Zhuang et al., 2001).

143 The methane dynamics module (MDM) (Zhuang et al., 2004) considers the processes of
144 methanogenesis, methanotrophy, and the transportation pathways including: (1) diffusion
145 through the soil profile; (2) plant-aided transportation; and (3) ebullition. The soil temperatures
146 calculated from STM, after interpolation into 1-cm sub-layers, are input to the MDM. The water-
147 table depth and soil water content in the unsaturated zone for methane production and emission
148 are obtained from HM, and NPP is calculated from the CNDM. Soil-water pH is prescribed from
149 observed data and the root distribution determines the redox potential (Zhuang et al., 2004).

150

151 **2.3 Model Parameterization**

152 We have parameterized the key parameters of the individual modules including HM,
153 STM, and MDM in Wang et al. (2016). The parameters in CNDM for upland soils and
154 vegetation have been optimized in the previous studies (Zhuang et al 2002, 2003; Tang and
155 Zhuang 2008). Here we parameterized P-TEM for peatland ecosystems using data from a
156 moderate rich *Sphagnum* spp. open fen (APEXCON) and a *Sphagnum*-black spruce (*Picea*
157 *mariana*) bog (APEXPER) (Table 1). Both are located in the Alaskan Peatland Experiment
158 (APEX) study area, where *Picea mariana* is the only tree species above breast height in
159 APEXPER. Three water table position manipulations were established in APEX including a
160 control, a lowered, and a raised water table plots (Chivers et al., 2009; Turetsky et al., 2008;

161 Kane et al., 2010; Churchill et al., 2011). There were also several internal collapse scars that
162 formed with thaw of surface permafrost, including a non-, an old, and a new collapse plots.
163 APEXCON represents the control manipulation and APEXPER represents the non-collapse plot.
164 The annual NPP and aboveground biomass at both sites have been measured in 2009. There were
165 no belowground observations at APEX, however at a Canadian peatland, Mer Bleue, which
166 includes *Sphagnum* spp. dominated bog (dominated by shrubs and *Sphagnum*) and pool fen
167 (dominated by sedges and herbs and *Sphagnum*). The belowground biomass was also observed at
168 Suurisuo mire complex, southern Finland, a sedge fen site dominated by *Carex rostrate*. We
169 used the ratio (70%) of belowground biomass to total biomass from these two study sites to
170 calculate the missing belowground biomass values at APEXCON and APEXPER (Table 2). We
171 conducted 100,000 Monte Carlo ensemble simulations to calibrate the model for each site using
172 a Bayesian approach and parameter values with the modes in their posterior distributions were
173 selected (Tang and Zhuang, 2008, 2009).

174

175 **2.4 Regional Model Input Data**

176 The Alaskan C stock was simulated through the Holocene driven with vegetation data
177 reconstructed for four time periods including a time period encompassing a millennial-scale
178 warming event during the last deglaciation known as the Bølling-Allerød at 15-11 ka (1 ka =
179 1000 cal yr Before Present), HTM during the early Holocene at 11-10 and 10-9 ka, and the mid-
180 (9-5 ka) and late- Holocene (5 ka-1900 AD) (He et al., 2014). We used the modern vegetation
181 distribution for the simulation during the period 1900-2000 AD (Figure 2). We assumed that the
182 vegetation distribution remained static within each corresponding time period. Upland

183 ecosystems were classified into boreal deciduous broadleaf forest, boreal evergreen needleleaf
184 and mixed forest, alpine tundra, wet tundra; and barren lands (Table 3). By using the same
185 vegetation distribution map, we reclassified the upland ecosystems into two peatland types
186 including *Sphagnum* spp. poor fens (SP) dominated by tundra and *Sphagnum* spp.-black spruce
187 (*Picea mariana*) bog/ peatland (SBP) dominated by forest ecosystems (Table 3).

188 Upland and peatland ecosystem distribution for each grid cell was determined using the
189 wetland inundation data extracted from the NASA/ GISS global natural wetland dataset
190 (Matthews and Fung, 1987). The resolution was resampled to $0.5^{\circ} \times 0.5^{\circ}$ from $1^{\circ} \times 1^{\circ}$. Given the
191 same topography of Alaska during the Holocene, we assumed that the wetland distribution kept
192 the same throughout the Holocene. The inundation fraction was assumed to be the same within
193 each grid through time and the land grids not covered by peatland were treated as uplands. We
194 calculated the total area of modern Alaskan peatlands to be $302,410 \text{ km}^2$, which was within the
195 range from $132,000 \text{ km}^2$ (Bridgham et al., 2006) to $596,000 \text{ km}^2$ (Kivinen and Pakarinen, 1981).
196 The soil water pH data were extracted from Carter and Scholes (2000), and the elevation data
197 were derived from Zhuang et al. (2007).

198 Our regional simulations considered the effects of basal ages on carbon accumulation. To
199 obtain the spatially explicit basal age data for all peatlands grid cells, we first categorized the
200 observed basal ages of peat samples from Gorham et al. (2012) into different time periods
201 including 15-11 ka, 11-10 ka, 10-9 ka, and 9 ka-19th (Figure 2). For each time period, the areas
202 dominated with different vegetation types were assigned with varying peatland basal ages. To do
203 that, we examined the association of peat basal ages and vegetation types from peat core data.
204 For instance, we found that peatland initiations during 15-11 ka occurred in the regions that were
205 dominated by alpine tundra at south, northwestern, and southeastern coast. We thus assign the

206 different peatland basal ages for the grid cells according to their vegetation types for each time
207 slice (Table 4).

208 Climate data were bias-corrected from ECBilt-CLIO model output (Timm and
209 Timmermann, 2007) to minimize the difference from CRU data (He et al., 2014). Climate fields
210 include monthly precipitation, monthly air temperature, monthly net incoming solar radiation,
211 and monthly vapor pressure at resolution of $2.5^{\circ} \times 2.5^{\circ}$. We used the same time-dependent
212 forcing atmospheric carbon dioxide concentration data for model input as were used in ECBilt-
213 CLIO transient simulations from the Taylor Dome (Timm and Timmermann, 2007). The
214 historical climate data used for the simulation through the 20th century were monthly CRU2.0
215 data (Mitchell et al., 2004).

216

217 **2.5 Simulations and Sensitivity Test**

218 Simulations for pixels located on the Kenai Peninsula from 15 to 5 ka were first
219 conducted with the parameterized model. The peat-core data from four peatlands on the Kenai
220 Peninsula, Alaska (Jones and Yu, 2010; Yu et al., 2010) (Table 5, also see Table 3 in Wang et al.
221 (2016)) were used to compare with the simulations. The observed data include the peat depth,
222 bulk density of both organic and inorganic matters at 1-cm interval, and age determinations. The
223 simulated C accumulation rates represent the actual (“true”) rates at different times in the past.
224 However, the calculated accumulation rates from peat cores are considered as “apparent”
225 accumulation rates, as peat would continue to decompose since the time of formation until
226 present when the measurement was made (Yu, 2012). To facilitate comparison between
227 simulated and observed accumulation rates, we converted the simulated “true” accumulation

228 rates to “apparent” rates, following the approach by Spahni et al. (2013). That is, we summed the
229 annual net C accumulation over each 500-year interval and deducted the total amount of C
230 decomposition from that time period, then dividing by 500 years.

231 Second, we conducted a transient regional simulation driven with monthly climatic data
232 (Figure 3) from 15 ka to 2000 AD. The simulation was conducted assuming all grid cells were
233 taken up by upland ecosystems to get the upland soil C spatial distributions during different time
234 periods. We then conducted the second simulation assuming all grid cells were dominated by
235 peatland ecosystems following Table 3 to obtain the distributions of peat SOC accumulation.
236 Finally, we used the inundation fraction map to extract both uplands and peatlands and estimated
237 the corresponding SOC stocks within each grid, which were then summed up to represent the
238 Alaskan SOC stock. We also used the observed mean C content of 46.8% in peat mass and bulk
239 density of $166 \pm 76 \text{ kg m}^{-3}$ in Alaska (Loisel et al., 2014) to estimate peat depth distribution from
240 the simulated peat SOC density (kg C m^{-2}).

241 Third, we conducted a series of extra simulations to further examine how uncertain
242 climates and vegetation distribution affect our results. We used the original forcing data as the
243 standard scenario and the warmer (monthly temperature $+5^\circ\text{C}$) and cooler (-5°C) as other two
244 scenarios while keeping the rest forcing data unchanged. Similarly, we used the original forcing
245 data as the standard scenario and the wetter (monthly precipitation $+10 \text{ mm}$) and drier (-10 mm)
246 to test the effect from precipitation. To further study if vegetation distribution has stronger
247 effects on SOC accumulation than climate in Alaska, we simply replaced SBP with SP and
248 replaced the upland forests with tundra at the beginning of 15 ka. We then conducted the
249 simulation under “warmer” and “wetter” conditions simultaneously as described before while
250 keeping the vegetation distribution unchanged.

251 3. Results and Discussion

252 3.1 Simulated Peatland Carbon Accumulation Rates at Site Level

253 Our paleo simulations showed a large peak of peat C accumulation rates at 11-9 ka
254 during the HTM (Figure 4). The simulated “true” and “apparent” rates captured this primary
255 feature in peat-core data at almost all sites (Jones and Yu, 2010; See Wang et al. (2016) Table 3
256 for sites details). We simulated an average of peat SOC “apparent” accumulation rate of 11.4
257 $\text{g C m}^{-2} \text{ yr}^{-1}$ from 15 to 5 ka, which was slightly higher than the observations at four sites
258 ($10.45 \text{ g C m}^{-2} \text{ yr}^{-1}$). The simulated rate during the HTM was $26.5 \text{ g C m}^{-2} \text{ yr}^{-1}$, up to five
259 times higher than the rest of the Holocene ($5.04 \text{ g C m}^{-2} \text{ yr}^{-1}$). This corresponded to the
260 observed average rate of $20 \text{ g C m}^{-2} \text{ yr}^{-1}$ from 11.5 to 8.6 ka, which is, four times higher than
261 $5 \text{ g C m}^{-2} \text{ yr}^{-1}$ over the rest of the Holocene.

262

263 3.2 Vegetation Carbon

264 Model simulations showed an overall low vegetation C before the HTM (15-11 ka)
265 (Figure 5a), paralleled to the relatively low annual and long-term NPP (Figures 5b and c). The
266 lowest amount of C ($\sim 0.8 \text{ kg C m}^{-2}$) was stored in *Sphagnum*-dominated peatland. *Sphagnum*-
267 black spruce peatland also had low vegetation C density ($\sim 1 \text{ kg C m}^{-2}$). Upland vegetation
268 showed a generally higher C storage, among which boreal evergreen needleleaf forest ranked the
269 first ($\sim 2 \text{ kg C m}^{-2}$). Highest NPP accompanied by highest vegetation carbon appeared during the
270 HTM (11-9 ka) (Figures 5a and b). Lower annual C uptake along with lower C was found during

271 mid- and late- Holocene (9 ka-19th), where peatland ecosystems exhibited the most obvious
272 drops (Figures 5a and b).

273 In general, vegetation held about 2 Pg C before the HTM (Figure 6). Upland tundra
274 ecosystems accounted for the most amount of C. During the HTM, Boreal evergreen needleleaf
275 forest reached its highest and had an overwhelming proportion over total C. Similarly, a peak of
276 total vegetation C appeared at the same time, averaging around 4.3 Pg C. Large decrease
277 occurred at the mid-Holocene and a slight decline continued till the late-Holocene. We estimated
278 a total 2.9 Pg C stored in modern Alaskan vegetation, with 0.4 Pg in peatlands and 2.5 Pg in non-
279 peatlands. The uncertainties during the model calibration (Table 2) resulted in 0.3-0.6 Pg C and
280 2.2-3.1 Pg C in peatlands (see Wang et al. (2016) for model parameters) and non-peatland
281 vegetation (see Tang and Zhuang (2008) for uncertainty analyses for upland vegetation),
282 respectively. Our estimation of 2.5-3.7 Pg C stored in the Alaskan vegetation was lower than the
283 previous estimate of 5 Pg (Balshi et al., 2007; McGuire et al., 2009), presumably due to the prior
284 ranges of model parameters used from Tang and Zhuang (2008). Our overestimation of peatland
285 area may also lead to a reduction of Alaskan non-peatland area.

286

287 **3.3 Soil Carbon**

288 Carbon storage in Alaskan non-peatland soils varied spatially (Figure 7). Moist tundra
289 had the highest SOC density (12-25 kg C m⁻²), followed by deciduous broadleaf forest (8-13
290 kg C m⁻²) and evergreen needleleaf forest (3-8 kg C m⁻²) through all time slices between 15 ka
291 and 2000 AD. Dramatic changes of vegetation types have occurred in Alaska during different
292 periods (Figure 2). Before the HTM (15-11 ka), the terrestrial ecosystem was dominated by

293 tundra. Northwestern coast and eastern interior was covered by moist tundra. Southwestern
294 Alaska and the interior south of the Brooks Range were dominated by alpine tundra (Figure 2a).
295 The basal ages of peat samples from Gorham et al. (2012) suggested that peatlands were likely to
296 form from the (alpine) tundra ecosystems, although patches of boreal deciduous broadleaf forest
297 and boreal evergreen needleleaf and mixed forest appeared at the north of the Alaska Range.
298 Initially, only *Sphagnum* open peatland (SP) existed, with less C ($<10 \text{ kg C m}^{-2}$) sequestered in
299 the southeastern Brooks Range in comparison with southwestern and northwestern coastal parts
300 ($>15 \text{ kg C m}^{-2}$) (Figure 8a). Approximately $4.5 \times 10^5 \text{ km}^2$ area was covered by peatlands at the
301 beginning of the HTM ($\sim 11 \text{ ka}$) (Figure 9). During the HTM (11-9 ka), boreal deciduous
302 broadleaf and boreal evergreen needleleaf and mixed forests expanded (Figures 8b and c).
303 Coastal tundra (moist wet tundra) covered north of the Brooks Range between 11 and 10 ka,
304 where SP continued its expansion (Figure 8b). *Sphagnum*-black spruce forested peatland began
305 forming in southwestern coast and eastern interior regions, with a rapid increase of total peatland
306 area to about $13 \times 10^5 \text{ km}^2$ (Figure 9). At 10-9 ka, boreal deciduous forest expanded to north of
307 the Brooks Range, making forest the dominant biome in Alaska (Figure 2c). Prevailing forest
308 ecosystems indicated a large expansion of peatland, with SBP covering the interior Alaska
309 (Figure 8c). During the mid-Holocene (9-5 ka), the terrestrial landscape generally resembled
310 present-day ecosystems (Bigelow et al., 2003). Boreal evergreen needleleaf and mixed forest
311 prevailed in southern and interior Alaska with tundra returned to north of the Brooks Range and
312 western Alaska (Figures 2d and e). Although SP kept forming towards west, some areas
313 dominated by SBP in interior Alaska ceased accumulating C (Figure 8d). At 5k-19th, almost all
314 the peatlands have formed, with some interior regions exhibiting a C loss (Figure 8e). C
315 accumulation increased again in the last century, averaging about $20 \text{ kg C m}^{-2} \text{ kyr}^{-1}$ (Figure 8f).

316 We found that the distribution of SOC densities of both upland and peatland varied greatly
317 depending on the vegetation distribution within each time slice, indicating that vegetation
318 composition might be a major factor controlling regional C dynamics.

319 An average peat SOC “apparent” accumulation rate of $13 \text{ g C m}^{-2}\text{yr}^{-1}$ (2.3 Tg C yr^{-1}
320 for the entire Alaska) was estimated from 15 ka to 2000 AD (Figure 10), lower than 18.6
321 $\text{g C m}^{-2}\text{yr}^{-1}$ as estimated from peat cores for northern peatlands (Yu et al., 2010), and slightly
322 higher than the observed rate of $13.2 \text{ g C m}^{-2}\text{yr}^{-1}$ from four peatlands in Alaska (Jones and Yu,
323 2010). A simulated peak occurred during the HTM with the rate $29.1 \text{ g C m}^{-2}\text{yr}^{-1}$ (5.1 Tg C
324 yr^{-1}), which was slightly higher than the observed $25 \text{ g C m}^{-2}\text{yr}^{-1}$ for northern peatlands and
325 $\sim 20 \text{ g C m}^{-2}\text{yr}^{-1}$ for Alaska (Yu et al., 2010). It was almost four times higher than the rate 6.9
326 $\text{g C m}^{-2}\text{yr}^{-1}$ (1.4 Tg C yr^{-1}) over the rest of the Holocene, which corresponded to the peat core-
327 based observations of $\sim 5 \text{ g C m}^{-2}\text{yr}^{-1}$. The mid- and late Holocene showed much slower C
328 accumulation at a rate approximately five folds lower than during the HTM. This corresponded
329 to the observation of a six-fold decrease in the rate of new peatland formation after 8.6 ka (Jones
330 and Yu 2010). The C accumulation rates increased abruptly to $39.2 \text{ g C m}^{-2}\text{yr}^{-1}$ during the last
331 century, within the field-measured average apparent rate range of $20\text{-}50 \text{ g C m}^{-2}\text{yr}^{-1}$ over the
332 last 2000 years (Yu et al., 2010).

333 The SOC stock of northern peatlands has been estimated in many studies, ranging from
334 210 to 621 Pg (Oechel 1989; Gorham 1991; Armentano and Menges, 1986; Turunen et al., 2002;
335 Yu et al., 2010; see Yu 2012 for a review). Assuming Alaskan peatlands were representative of
336 northern peatlands and using the area of Alaskan peatlands ($0.45 \times 10^6 \text{ km}^2$; Kivinen and
337 Pakarinen, 1981) divided by the total area of northern peatlands ($\sim 4 \times 10^6 \text{ km}^2$; Maltby and

338 Immirzi 1993), we estimated a SOC stock of 23.6-69.9 Pg C for Alaskan peatlands. Our model
339 estimated 27-48 Pg C (23.9 Pg C in SP and 13.5 Pg C in SBP) had been accumulated from 15 ka
340 to 2000 AD (Figure 11), due to uncertain parameters (Table 2, see Wang et al. (2016) for model
341 parameters). The uncertainty can also be resulted from peat basal age distributions and the
342 estimation of total peatland area using modern inundation data as discussed above. By
343 incorporating the observed basal age distribution to determine the expansion of peatland through
344 time, we estimated that approximately 68% of Alaskan peatlands had formed by the end of the
345 HTM, similar to the estimation from observed basal peat ages that 75% peatlands have formed
346 by 8.6 ka (Jones and Yu 2010).

347 The northern circumpolar soils were estimated to cover approximately $18.78 \times 10^6 \text{ km}^2$
348 (Tarnocai et al., 2009). The non-peatland soil C stock was estimated to be in the range of 150-
349 191 Pg C for boreal forests (Apps et al., 1993; Jobbagy and Jackson, 2000), and 60-144 Pg C for
350 tundra in the 0-100 cm depth (Apps et al., 1993; Gilmanov and Oechel, 1995; Oechel et al.,
351 1993). $1.24 \times 10^6 \text{ km}^2$ non-peatland area was estimated from the total land area of Alaska
352 ($1.69 \times 10^6 \text{ km}^2$). Therefore, Alaska non-peatland soil contained 17-27 Pg C by using the ratio of
353 Alaskan over northern non-peatland. In comparison, we modeled 9-15 Pg C (within 1-meter
354 depth), depending on the prior ranges of model parameters from Tang and Zhuang (2008).

355 The simulated modern SOC distribution (Figure 12c) was largely consistent with the
356 study of Hugelius et al. (2014) (see Figure 3 in the paper). The model captured the SOC density
357 on northern and southwestern coasts of Alaska with most grids $>40 \text{ kg C m}^{-2}$ on average. Those
358 regions also showed high SOC density ($>75 \text{ kg C m}^{-2}$), which was also exhibited in our result.
359 East part and west coast had the lowest SOC densities, corresponding to the simulation result that
360 most grids had SOC values between 20 and 40 kg C m^{-2} . We estimated an average peat depth of

361 1.9±0.8 m considering the uncertainties within dry bulk densities. It was similar to the observed
362 mean depth of 2.29 m for Alaskan peatlands (Gorham et al., 1991, 2012). Our estimates (Figure
363 12d) showed a relatively high correlation with the 64 observed peat samples, especially with
364 higher depths (Figure 13) ($R^2 = 0.45$). The large intercept of the regression line (101 cm)
365 suggested that the model might have not performed well in estimating the grids with low peat
366 depths (<50 cm). The peat characteristics (e.g., bulk density) from location to location may differ
367 largely, even if within the same small region. Thus, it is difficult to capture the observed
368 variations of peat depths as we used the averaged bulk density of whole Alaska.

369 **3.4 Effects of Climate on Ecosystem Carbon Accumulation**

370 The simulated climate by ECBilt-CLIO model showed that among the six time periods, the
371 coolest temperature appeared at 15-11 ka, followed by the mid- and late- Holocene (5 ka-1900
372 AD). Those two periods were also generally dry (Figure 3f). The former represented colder and
373 drier climate before the onset of the Holocene and the HTM (Barber and Finney, 2000; Edwards
374 et al., 2001). The latter represented post-HTM neoglacial cooling, which has caused permafrost
375 aggradation across northern high latitudes (Oksanen et al., 2001; Zoltai, 1995).

376 Despite the relatively large inter-annual NPP variation resulted from the annual
377 fluctuations of the climate forcing (Figure 5b), the long-term NPP, vegetation C density and
378 storage were highest during the HTM (Figures 5a and c). Annual C accumulation rates also
379 reached the highest (Figures 5-11). The long-term variation of NPP has a similar pattern of the
380 climate (see Figure 3 for climate variables), where higher NPP, along with higher vegetation C
381 coincided with warmer temperatures and enhanced precipitation during the HTM, compared to
382 other time periods. ECBilt-CLIO simulated a warmest summer and a prolonged growing season,

383 leading to a stronger seasonality of temperature during the HTM (Kaufman et al., 2004, 2016), in
384 line with the orbitally-induced maximum summer insolation (Berger and Loutre, 1991; Renssen
385 et al., 2009). The coincidence between the highest vegetation C uptake and SOC accumulation
386 rates and the warmest summer and the wetter-than-before conditions indicated a strong link
387 between those climate variables and C dynamics in Alaska. Enhanced climate seasonality
388 characterized by warmer summer, enhanced summer precipitation and possibly earlier snow melt
389 during the HTM accelerated the photosynthesis and subsequently increased NPP (Tucker et al.,
390 2001; Kimball et al., 2004; Linderholm, 2006). As shown in our sensitivity test, annual NPP was
391 increased by 40 and 20 g C m⁻² yr⁻¹ under the warmer and wetter scenarios, respectively
392 (Figures 14a, b). Meanwhile, warmer condition could positively affect the SOC decomposition
393 (Nobrega et al., 2007). However, it could be offset to a certain extent via the hydrological effect,
394 as higher precipitation could raise the water-table position, allowing less space for aerobic
395 heterotrophic respiration. Our sensitivity test results indicated that warmer and wetter conditions
396 could lead to an increase of decomposition up to 35 and 15 g C m⁻² yr⁻¹, respectively (Figures
397 14c, d). We did not find a decrease in total heterotrophic respiration throughout Alaska from the
398 higher precipitation. It was presumably due to a much larger area of upland soils (1.3 ×10⁶ km²)
399 than peatland soils (0.26 ×10⁶ km²), as higher precipitation would cause higher aerobic
400 respiration in the unsaturated zone of upland soils, and consequently stimulated the SOC
401 decomposition. The relatively low NPP and vegetation C density, along with the lower total soil
402 C stocks were consistent with the unfavorable cool and dry climate conditions at 15-11 ka and
403 during the mid- and late- Holocene. Statistical analysis indicated that temperature had the most
404 significant effect on peat SOC accumulation rate, followed by the seasonality of NIRR (Wang et
405 al., 2016). The seasonality of temperature, the interaction of temperature and precipitation, and

406 precipitation alone also showed significance. The strong link between climate factors and C
407 dynamics may explain the lower SOC accumulation during the neoglacier cooling period
408 (Marcott et al., 2013; Vitt et al., 2000; Peteet et al., 1998; Yu et al. 2010). The rapid peat SOC
409 accumulation during the 20th century under warming and wetter climate may suggest a
410 continuous C sink in this century, as concluded in Spahni et al. (2013). However, the rising
411 temperature in the future may have positive effects on heterotrophic respiration and
412 simultaneously increase evapotranspiration and lower water table. This could increase aerobic
413 decomposition and thus switch the Alaskan peatland from a C sink into a C source. Moreover,
414 the increasing anthropogenic activities including land use will probably increase drought and
415 subsequently enhance the risk of fire, releasing carbon to the atmosphere. The fate of Alaskan
416 SOC stock and the biogeochemical cycling of the terrestrial ecosystems under future scenarios
417 need further investigation.

418

419 **3.5 Effects of Vegetation Distribution on Ecosystem Carbon Accumulation**

420 Climate variables significantly affect C dynamics within each time slice. However,
421 different vegetation distributions during various periods led to clear step changes, suggesting
422 vegetation composition was likely to be another primary factor (Figures 6, 7, 8, and 11). As key
423 parameters controlling C dynamics in the model (e.g., maximum rate of photosynthesis, litter fall
424 C, maximum rate of monthly NPP) are ecosystem type specific, vegetation distribution changes
425 may drastically affect regional plant productivity and C storage. Our sensitivity test indicated
426 that by replacing all vegetation types with forests, there was a total increase of 36.9 Pg in upland
427 plus peatland soils. There was also an increase of 48.8 Pg C under warmer and wetter conditions,

428 suggesting that both climate and vegetation distribution may have played important roles in
429 carbon accumulation.

430 The vegetation changes reconstructed from fossil pollen data during different time
431 periods followed the general climate history during the last 15,000 years. For instance, the
432 migration of dark boreal forests over snow-covered tundra during the HTM was probably
433 induced by the warmer and wetter climate resulted from the insolation changes (He et al., 2014).
434 The cooler and drier climate after the mid-Holocene limited the growth of boreal broadleaf
435 conifers (Prentice et al., 1992), and therefore resulted in the replacement of broadleaf forest with
436 needleleaf forest and tundra ecosystems. Since the parameters of our model for individual
437 vegetation type were static, parameterizing the model using modern site-level observations might
438 have introduced uncertainty to parameters, which may result in regional simulation uncertainties.
439 Assuming each parameter as constant (e.g. the lowest water-table boundary, see Wang et al.
440 (2016) for details) over time may also weaken the model's response to different climate
441 scenarios. Furthermore, applying static vegetation maps at millennial scales and using modern
442 elevation and pH data may simplify the complicated changes of landscape and terrestrial
443 ecosystems, as vegetation can shift within hundreds of years (Ager and Brubake, 1985; see He et
444 al. (2014) discussion section). Relatively coarse spatial resolution ($0.5^{\circ}\times 0.5^{\circ}$) in P-TEM
445 simulations may also introduce uncertainties. In addition, because we used the modern
446 inundation map to delineate the peatland and upland within each grid cell, we might have
447 overestimated the total peatland area since not all inundated areas are peatlands. Linking field-
448 estimated basal ages of peat cores to the vegetation types during each period involves large
449 uncertainties due to the limitation of the peat classification and insufficient peat samples. Thus,

450 the estimated spatially explicit basal age data shall also introduce a large uncertainty to our
451 regional quantification of carbon accumulation.

452

453 **4. Conclusions**

454 We used a biogeochemistry model for both peatland and non-peatland ecosystems to
455 quantify the C stock and its changes over time in Alaskan terrestrial ecosystems during the last
456 15,000 years. The simulated peat SOC accumulation rates were compared with peat-core data
457 from four peatlands on the Kenai Peninsula in southern Alaska. The model well estimated the
458 peat SOC accumulation rates trajectory throughout the Holocene. Our regional simulation
459 showed that 36-63 Pg C had been accumulated in Alaskan land ecosystems since 15,000 years
460 ago, including 27-48 Pg C in peatlands and 9-15 Pg C in non-peatlands (within 1 m depth). We
461 also estimated that 2.5-3.7 Pg C was stored in contemporary Alaskan vegetation, with 0.3-0.6 Pg
462 C in peatlands and 2.2-3.1 Pg C in non-peatlands. The estimated average rate of peat C
463 accumulation was 2.3 Tg C yr⁻¹ with a peak (5.1 Pg C yr⁻¹) in the Holocene Thermal
464 Maximum (HTM), four folds higher than the rate of 1.4 Pg C yr⁻¹ over the rest of the Holocene.
465 The 20th century represented another high SOC accumulation period after a much low
466 accumulation period of the late Holocene. We estimated an average depth of 1.9 m of peat in
467 current Alaskan peatlands, similar to the observed mean depth. The changes of vegetation
468 distribution were found to be the major control on the spatial variations of SOC accumulation in
469 different time periods. The warming in the HTM characterized by the increased summer
470 temperature and increased seasonality of solar radiation, as well as the higher precipitation might
471 have played an important role in the high C accumulation.

472 **5. Acknowledgment.** We acknowledge the funding support from a NSF project IIS-1027955
473 and a DOE project DE-SC0008092. We also acknowledge the SPRUCE project to allow us use
474 its data. Data presented in this paper are publicly accessible: ECBilt-CLIO Paleosimulation
475 (<http://apdrc.soest.hawaii.edu/datadoc/sim2bl.php>), CRU2.0 (<http://www.cru.uea.ac.uk/data>).
476 Model parameter data and model evaluation process are in Wang et al. (2016). Other simulation
477 data including model codes are available upon request from the corresponding author
478 (qzhuang@purdue.edu).

479

480 **6. References**

- 481 Ager, T. A., & Brubaker, L.: Quaternary palynology and vegetational history of Alaska. Pollen
482 Records of Late Quaternary North American Sediments, 353-384, 1985.
- 483 Apps, M. J., Kurz, W. A., Luxmoore, R. J., Nilsson, L. O., Sedjo, R. A., Schmidt, R., ... &
484 Vinson, T. S.: Boreal forests and tundra. Water, Air, and Soil Pollution, 70(1-4), 39-53, 1993.
- 485 Armentano, T. V., & Menges, E. S.: Patterns of change in the carbon balance of organic soil-
486 wetlands of the temperate zone. The Journal of Ecology, 755-774, 1986.
- 487 Assessment, A. C. I.: Forests, land management and agriculture. Arctic Climate Impact
488 Assessment, 781-862, 2005.
- 489 Balshi, M. S., McGuire, A. D., Zhuang, Q., Melillo, J., Kicklighter, D. W., Kasischke, E., ... &
490 Burnside, T. J.: The role of historical fire disturbance in the carbon dynamics of the pan-boreal
491 region: A process-based analysis. Journal of Geophysical Research: Biogeosciences, 112(G2),
492 2007.
- 493 Barber, V. A., & Finney, B. P.: Late Quaternary paleoclimatic reconstructions for interior Alaska
494 based on paleolake-level data and hydrologic models. Journal of Paleolimnology, 24(1), 29-41,
495 2000.
- 496 Belyea, L. R.: Nonlinear dynamics of peatlands and potential feedbacks on the climate
497 system. Carbon cycling in northern peatlands, 5-18, 2009.
- 498 Berger, A., & Loutre, M. F.: Insolation values for the climate of the last 10 million
499 years. Quaternary Science Reviews, 10(4), 297-317, 1991.
- 500 Bigelow, N. H., Brubaker, L. B., Edwards, M. E., Harrison, S. P., Prentice, I. C., Anderson, P.
501 M., ... & Kaplan, J. O.: Climate change and Arctic ecosystems: 1. Vegetation changes north of
502 55 N between the last glacial maximum, mid-Holocene, and present. Journal of Geophysical
503 Research: Atmospheres, 108(D19), 2003.
- 504 Bridgham, S. D., Megonigal, J. P., Keller, J. K., Bliss, N. B., & Trettin, C.: The carbon balance
505 of North American wetlands. Wetlands, 26(4), 889-916, 2006.
- 506 Carter, A. J., & Scholes, R. J.: SoilData v2. 0: generating a global database of soil
507 properties. Environmentek CSIR, Pretoria, South Africa, 2000.

508 Change, I. C.: Mitigation of Climate Change. Contribution of Working Group III to the Fifth
509 Assessment Report of the Intergovernmental Panel on Climate Change. Cambridge University
510 Press, Cambridge, UK and New York, NY, 2014.

511 Change, I. C.: The Physical Science Basis: Working Group I Contribution to the Fifth
512 Assessment Report of the Intergovernmental Panel on Climate Change. New York: Cambridge
513 University Press, 1, 535-1, 2013.

514 Chivers, M. R., Turetsky, M. R., Waddington, J. M., Harden, J. W., & McGuire, A. D.: Effects
515 of experimental water table and temperature manipulations on ecosystem CO₂ fluxes in an
516 Alaskan rich fen. *Ecosystems*, 12(8), 1329-1342, 2009.

517 Churchill, A.: The response of plant community structure and productivity to changes in
518 hydrology in Alaskan boreal peatlands. Master Thesis, University of Alaska, Fairbanks, AK,
519 USA. 119 pp, 2011.

520 Conrad, R.: Contribution of hydrogen to methane production and control of hydrogen
521 concentrations in methanogenic soils and sediments. *FEMS Microbiology Ecology*, 28(3), 193-
522 202, 1999.

523 Davidson, E. A., & Janssens, I. A.: Temperature sensitivity of soil carbon decomposition and
524 feedbacks to climate change. *Nature*, 440(7081), 165-173, 2006.

525 Davidson, E. A., Trumbore, S. E., & Amundson, R.: Biogeochemistry: soil warming and organic
526 carbon content. *Nature*, 408(6814), 789-790, 2000.

527 Edwards, M. E., Mock, C. J., Finney, B. P., Barber, V. A., & Bartlein, P. J.: Potential analogues
528 for paleoclimatic variations in eastern interior Alaska during the past 14,000 yr: atmospheric-
529 circulation controls of regional temperature and moisture responses. *Quaternary Science*
530 *Reviews*, 20(1), 189-202, 2001.

531 Euskirchen, E. S., McGuire, A. D., & Chapin, F. S.: Energy feedbacks of northern high-latitude
532 ecosystems to the climate system due to reduced snow cover during 20th century
533 warming. *Global Change Biology*, 13(11), 2425-2438, 2007.

534 Frohking, S., Roulet, N. T., Tuittila, E., Bubier, J. L., Quillet, A., Talbot, J., & Richard, P. J. H.:
535 A new model of Holocene peatland net primary production, decomposition, water balance, and
536 peat accumulation. *Earth System Dynamics*, 1(1), 1-21, 2010.

537 Frohking, S., Talbot, J., Jones, M. C., Treat, C. C., Kauffman, J. B., Tuittila, E. S., & Roulet, N.:
538 Peatlands in the Earth's 21st century climate system. *Environmental Reviews*, 19(NA), 371-396,
539 2011.

540 Gilmanov, T. G., & Oechel, W. C.: New estimates of organic matter reserves and net primary
541 productivity of the North American tundra ecosystems. *Journal of Biogeography*, 22, 723-741, 1995.

542 Gorham, E. V. I. L. E.: Biotic impoverishment in northern peatlands. *The earth in transition:*
543 *patterns and processes of biotic impoverishment.* Cambridge University Press, Cambridge, UK,
544 65-98, 1990.

545 Gorham, E., Lehman, C., Dyke, A., Clymo, D., & Janssens, J.: Long-term carbon sequestration
546 in North American peatlands. *Quaternary Science Reviews*, 58, 77-82, 2012.

547 Gorham, E.: Northern peatlands: role in the carbon cycle and probable responses to climatic
548 warming. *Ecological applications*, 1(2), 182-195, 1991.

549 He, Y., Jones, M. C., Zhuang, Q., Bochicchio, C., Felzer, B. S., Mason, E., & Yu, Z.: Evaluating
550 CO₂ and CH₄ dynamics of Alaskan ecosystems during the Holocene Thermal
551 Maximum. *Quaternary Science Reviews*, 86, 63-77, 2014.

552 Hinzman, L. D., Viereck, L. A., Adams, P. C., Romanovsky, V. E., & Yoshikawa, K.: Climate
553 and permafrost dynamics of the Alaskan boreal forest. *Alaska's Changing Boreal Forest*, 39-61,
554 2006.

555 Hobbie, S. E.: Interactions between litter lignin and nitrogen litter lignin and soil nitrogen
556 availability during leaf litter decomposition in a Hawaiian montane forest. *Ecosystems*, 3(5),
557 484-494, 2000.

558 Hugelius, G., Strauss, J., Zubrzycki, S., Harden, J. W., Schuur, E., Ping, C. L., ... & O'Donnell, J.
559 A.: Estimated stocks of circumpolar permafrost carbon with quantified uncertainty ranges and
560 identified data gaps. *Biogeosciences*, 11(23), 6573-6593, 2014.

561 Jobbágy, E. G., & Jackson, R. B.: The vertical distribution of soil organic carbon and its relation
562 to climate and vegetation. *Ecological applications*, 10(2), 423-436, 2000.

563 Jones, M. C., & Yu, Z.: Rapid deglacial and early Holocene expansion of peatlands in
564 Alaska. *Proceedings of the National Academy of Sciences*, 107(16), 7347-7352, 2010.

565 Jones, P. D., & Moberg, A.: Hemispheric and large-scale surface air temperature variations: An
566 extensive revision and an update to 2001. *Journal of Climate*, 16(2), 206-223, 2003.

567 Kane, E. S., Turetsky, M. R., Harden, J. W., McGuire, A. D., & Waddington, J. M.: Seasonal ice
568 and hydrologic controls on dissolved organic carbon and nitrogen concentrations in a boreal-rich
569 fen. *Journal of Geophysical Research: Biogeosciences*, 115(G4), 2010.

570 Kaufman, D. S., Ager, T. A., Anderson, N. J., Anderson, P. M., Andrews, J. T., Bartlein, P. J., ...
571 & Dyke, A. S.: Holocene thermal maximum in the western Arctic (0–180 W). *Quaternary
572 Science Reviews*, 23(5), 529-560, 2004.

573 Kaufman, D.S., Axford, Y.L., Henerson, A., McKay, N.P., Oswald, W.W., Saenger, C.,
574 Anderson, R.S., Bailey, H.L., Clegg, B., Gajewski, K., Hu, F.S., Jones, M.C., Massa, C.,
575 Routson, C.C., Werner, A., Wooller, M.J., Yu, Z.: Holocene climate changes in eastern Beringia
576 (NW North America) e a systemic review of multi-proxy evidence. *Quaternary Science Reviews*,
577 this volume. <http://dx.doi.org/10.1016/j.quascirev.2015.10.021>, 2016.

578 Keller, J. K., & Bridgman, S. D.: Pathways of anaerobic carbon cycling across an ombrotrophic–
579 minerotrophic peatland gradient, 2007.

580 Keller, J. K., & Takagi, K. K.: Solid-phase organic matter reduction regulates anaerobic
581 decomposition in bog soil. *Ecosphere*, 4(5), 1-12, 2013.

582 Kimball, J. S., McDonald, K. C., Running, S. W., & Frohking, S. E.: Satellite radar remote
583 sensing of seasonal growing seasons for boreal and subalpine evergreen forests. *Remote Sensing
584 of Environment*, 90(2), 243-258, 2004.

585 Kivinen, E., and P. Pakarinen.: Geographical distribution of peat resources and major peatland
586 complex types in the world. *Annales Academiae Scientiarum Fennicae, Series A, Number 132*,
587 1981.

588 Kleinen, T., Brovkin, V., & Schuldt, R. J.: A dynamic model of wetland extent and peat
589 accumulation: results for the Holocene. *Biogeosciences*, 9(1), 235-248, 2012.

590 Kuhry, P., & Vitt, D. H.: Fossil carbon/nitrogen ratios as a measure of peat
591 decomposition. *Ecology*, 77(1), 271-275, 1996.

592 Linderholm, H. W.: Growing season changes in the last century. *Agricultural and Forest
593 Meteorology*, 137(1), 1-14, 2006.

594 Loisel, J., Gallego-Sala, A. V., & Yu, Z.: Global-scale pattern of peatland Sphagnum growth
595 driven by photosynthetically active radiation and growing season length. *Biogeosciences*, 9(7),
596 2737-2746, 2012.

597 Loisel, J., Yu, Z., Beilman, D. W., Camill, P., Alm, J., Amesbury, M. J., ... & Belyea, L. R.: A
598 database and synthesis of northern peatland soil properties and Holocene carbon and nitrogen
599 accumulation. the Holocene, 0959683614538073, 2014.

600 Maltby, E., & Immirzi, P.: Carbon dynamics in peatlands and other wetland soils regional and
601 global perspectives. *Chemosphere*, 27(6), 999-1023, 1993.

602 Manabe, S., & Wetherald, R. T.: On the distribution of climate change resulting from an increase
603 in CO₂ content of the atmosphere. *Journal of the Atmospheric Sciences*, 37(1), 99-118, 1980.

604 Manabe, S., & Wetherald, R. T.: Reduction in summer soil wetness induced by an increase in
605 atmospheric carbon dioxide. *Science*, 232(4750), 626-628, 1986.

606 Marcott, S. A., Shakun, J. D., Clark, P. U., & Mix, A. C.: A reconstruction of regional and global
607 temperature for the past 11,300 years. *science*, 339(6124), 1198-1201, 2013.

608 Matthews, E., & Fung, I.: Methane emission from natural wetlands: Global distribution, area,
609 and environmental characteristics of sources. *Global biogeochemical cycles*, 1(1), 61-86, 1987.

610 McGuire, A. D., & Hobbie, J. E.: Global climate change and the equilibrium responses of carbon
611 storage in arctic and subarctic regions. In *Modeling the Arctic system: A workshop report on the
612 state of modeling in the Arctic System Science program*, pp. 53-54, 1997.

613 McGuire, A. D., Anderson, L. G., Christensen, T. R., Dallimore, S., Guo, L., Hayes, D. J., ... &
614 Roulet, N.: Sensitivity of the carbon cycle in the Arctic to climate change. *Ecological
615 Monographs*, 79(4), 523-555, 2009.

616 McGuire, A. D., Melillo, J. M., Kicklighter, D. W., & Joyce, L. A.: Equilibrium responses of soil
617 carbon to climate change: empirical and process-based estimates. *Journal of Biogeography*, 785-
618 796, 1995.

619 Melillo, J. M., Kicklighter, D. W., McGuire, A. D., Peterjohn, W. T., & Newkirk, K.: Global
620 change and its effects on soil organic carbon stocks. In *Dahlem Conference Proceedings*, John
621 Wiley and Sons, New York, John Wiley & Sons, Ltd., Chichester, pp. 175-189, 1995.

622 Mitchell, T. D., Carter, T. R., Jones, P. D., Hulme, M., & New, M.: A comprehensive set of
623 high-resolution grids of monthly climate for Europe and the globe: the observed record (1901–
624 2000) and 16 scenarios (2001–2100). *Tyndall centre for climate change research working
625 paper*, 55(0), 25, 2004.

626 Moore, T. R., Bubier, J. L., Frolking, S. E., Lafleur, P. M., & Roulet, N. T.: Plant biomass and
627 production and CO₂ exchange in an ombrotrophic bog. *Journal of Ecology*, 90(1), 25-36, 2002.

628 Nobrega, S., & Grogan, P.: Deeper snow enhances winter respiration from both plant-associated
629 and bulk soil carbon pools in birch hummock tundra. *Ecosystems*, 10(3), 419-431, 2007.

630 Oechel, W. C., Hastings, S. J., Vourlitis, G., Jenkins, M., Riechers, G., & Grulke, N.: Recent
631 change of Arctic tundra ecosystems from a net carbon dioxide sink to a
632 source. *Nature*, 361(6412), 520-523, 1993.

633 Oechel, W. C.: Nutrient and water flux in a small arctic watershed: an overview. *Holarctic
634 Ecology*, 229-237, 1989.

635 Oksanen, P. O., Kuhry, P., & Alekseeva, R. N.: Holocene development of the Rogovaya river
636 peat plateau, European Russian Arctic. *The Holocene*, 11(1), 25-40, 2001.

637 Peteet, D., Andreev, A., Bardeen, W., & Mistretta, F.: Long-term Arctic peatland dynamics,
638 vegetation and climate history of the Pur-Taz region, western Siberia. *Boreas*, 27(2), 115-126,
639 1998.

640 Prentice, I. C., Cramer, W., Harrison, S. P., Leemans, R., Monserud, R. A., & Solomon, A. M.:
641 Special paper: a global biome model based on plant physiology and dominance, soil properties
642 and climate. *Journal of biogeography*, 117-134, 1992.

643 Raich, J. W., Rastetter, E. B., Melillo, J. M., Kicklighter, D. W., Steudler, P. A., Peterson, B.
644 J., ... & Vorosmarty, C. J.: Potential net primary productivity in South America: application of a
645 global model. *Ecological Applications*, 1(4), 399-429, 1991.

646 Renssen, H., Seppä, H., Heiri, O., Roche, D. M., Goosse, H., & Fichetef, T.: The spatial and
647 temporal complexity of the Holocene thermal maximum. *Nature Geoscience*, 2(6), 411-414,
648 2009.

649 Roulet, N. T., Lafleur, P. M., Richard, P. J., Moore, T. R., Humphreys, E. R., & Bubier, J. I. L.
650 L.: Contemporary carbon balance and late Holocene carbon accumulation in a northern
651 peatland. *Global Change Biology*, 13(2), 397-411, 2007.

652 Saarinen, T.: Biomass and production of two vascular plants in a boreal mesotrophic
653 fen. *Canadian Journal of Botany*, 74(6), 934-938, 1996.

654 Schuur, E. A., Bockheim, J., Canadell, J. G., Euskirchen, E., Field, C. B., Goryachkin, S. V., ...
655 & Mazhitova, G.: Vulnerability of permafrost carbon to climate change: implications for the
656 global carbon cycle. *BioScience*, 58(8), 701-714, 2008.

657 Sitch, S., Smith, B., Prentice, I. C., Arneth, A., Bondeau, A., Cramer, W., ... & Thonicke, K.:
658 Evaluation of ecosystem dynamics, plant geography and terrestrial carbon cycling in the LPJ
659 dynamic global vegetation model. *Global Change Biology*, 9(2), 161-185, 2003.

660 Spahni, R., Joos, F., Stocker, B. D., Steinacher, M., & Yu, Z. C.: Transient simulations of the
661 carbon and nitrogen dynamics in northern peatlands: from the Last Glacial Maximum to the 21st
662 century. *Climate of the Past*, 9(3), 1287-1308, 2013.

663 Stocker, B. D., Spahni, R., & Joos, F.: DYPTOP: a cost-efficient TOPMODEL implementation
664 to simulate sub-grid spatio-temporal dynamics of global wetlands and peatlands. *Geoscientific*
665 *Model Development*, 7(6), 3089-3110, 2014.

666 Stocker, B. D., Strassmann, K., & Joos, F.: Sensitivity of Holocene atmospheric CO₂ and the
667 modern carbon budget to early human land use: analyses with a process-based
668 model. *Biogeosciences*, 8(1), 69-88, 2011.

669 Tang, J., & Zhuang, Q.: A global sensitivity analysis and Bayesian inference framework for
670 improving the parameter estimation and prediction of a process-based Terrestrial Ecosystem
671 Model. *Journal of Geophysical Research: Atmospheres*, 114(D15), 2009.

672 Tang, J., & Zhuang, Q.: Equifinality in parameterization of process-based biogeochemistry
673 models: A significant uncertainty source to the estimation of regional carbon dynamics. *Journal*
674 *of Geophysical Research: Biogeosciences*, 113(G4), 2008.

675 Tang, J., Zhuang, Q., Shannon, R. D., & White, J. R.: Quantifying wetland methane emissions
676 with process-based models of different complexities. *Biogeosciences*, 7(11), 3817-3837, 2010.

677 Tarnocai, C., Canadell, J. G., Schuur, E. A. G., Kuhry, P., Mazhitova, G., & Zimov, S.: Soil
678 organic carbon pools in the northern circumpolar permafrost region. *Global biogeochemical*
679 *cycles*, 23(2), 2009.

680 Timm, O., & Timmermann, A.: Simulation of the Last 21 000 Years Using Accelerated
681 Transient Boundary Conditions*. *Journal of Climate*, 20(17), 4377-4401, 2007.

682 Tucker, C. J., Slayback, D. A., Pinzon, J. E., Los, S. O., Myneni, R. B., & Taylor, M. G.: Higher
683 northern latitude normalized difference vegetation index and growing season trends from 1982 to
684 1999. *International journal of biometeorology*, 45(4), 184-190, 2001.

685 Turetsky, M. R., Treat, C. C., Waldrop, M. P., Waddington, J. M., Harden, J. W., & McGuire, A.
686 D.: Short-term response of methane fluxes and methanogen activity to water table and soil
687 warming manipulations in an Alaskan peatland. *Journal of Geophysical Research:*
688 *Biogeosciences*, 113(G3), 2008.

689 Turunen, J., Tomppo, E., Tolonen, K., & Reinikainen, A.: Estimating carbon accumulation rates
690 of undrained mires in Finland—application to boreal and subarctic regions. *The Holocene*, 12(1),
691 69-80, 2002.

692 Vitt, D. H., Halsey, L. A., Bauer, I. E., & Campbell, C.: Spatial and temporal trends in carbon
693 storage of peatlands of continental western Canada through the Holocene. *Canadian Journal of*
694 *Earth Sciences*, 37(5), 683-693, 2000.

695 Wang, S., Zhuang, Q., Yu, Z., Bridgman, S., & Keller, J. K.: Quantifying peat carbon
696 accumulation in Alaska using a process-based biogeochemistry model, *Journal of Geophysical*
697 *Research: Biogeosciences*, 121, doi: 10.1002/2016JG003452, 2016.

698 XU-RI and PRENTICE, I. C.: Terrestrial nitrogen cycle simulation with a dynamic global
699 vegetation model. *Global Change Biology*, 14: 1745–1764. doi:10.1111/j.1365-
700 2486.2008.01625.x, 2008.

701 Yu, Z. C.: Northern peatland carbon stocks and dynamics: a review. *Biogeosciences*, 9(10),
702 4071-4085, 2012.

703 Yu, Z., Beilman, D. W., & Jones, M. C.: Sensitivity of northern peatland carbon dynamics to
704 Holocene climate change. *Carbon cycling in northern peatlands*, 55-69, 2009.

705 Yu, Z., Loisel, J., Brosseau, D. P., Beilman, D. W., & Hunt, S. J.: Global peatland dynamics
706 since the Last Glacial Maximum. *Geophysical Research Letters*, 37(13), 2010.

707 Zhuang, Q., McGuire, A. D., Melillo, J. M., Clein, J. S., Dargaville, R. J., Kicklighter, D. W., ...
708 & Hobbie, J. E.: Carbon cycling in extratropical terrestrial ecosystems of the Northern
709 Hemisphere during the 20th century: a modeling analysis of the influences of soil thermal
710 dynamics. *Tellus B*, 55(3), 751-776, 2003.

711 Zhuang, Q., McGuire, A. D., O'Neill, K. P., Harden, J. W., Romanovsky, V. E., & Yarie, J.:
712 Modeling soil thermal and carbon dynamics of a fire chronosequence in interior Alaska. *Journal*
713 *of Geophysical Research: Atmospheres*, 107(D1), 2002.

714 Zhuang, Q., Melillo, J. M., Kicklighter, D. W., Prinn, R. G., McGuire, A. D., Steudler, P. A., ...
715 & Hu, S.: Methane fluxes between terrestrial ecosystems and the atmosphere at northern high
716 latitudes during the past century: A retrospective analysis with a process-based biogeochemistry
717 model. *Global Biogeochemical Cycles*, 18(3), 2004.

718 Zhuang, Q., Melillo, J. M., McGuire, A. D., Kicklighter, D. W., Prinn, R. G., Steudler, P. A., ...
719 & Hu, S.: Net emissions of CH₄ and CO₂ in Alaska: Implications for the region's greenhouse
720 gas budget. *Ecological Applications*, 17(1), 203-212, 2007.

721 Zhuang, Q., Romanovsky, V. E., & McGuire, A. D.: Incorporation of a permafrost model into a
722 large-scale ecosystem model: Evaluation of temporal and spatial scaling issues in simulating soil
723 thermal dynamics. *Journal of Geophysical Research: Atmospheres*, 106(D24), 33649-33670,
724 2001.

725 Zhuang, Q., Zhu, X., He, Y., Prigent, C., Melillo, J. M., McGuire, A. D., ... & Kicklighter, D. W.:
726 Influence of changes in wetland inundation extent on net fluxes of carbon dioxide and methane
727 in northern high latitudes from 1993 to 2004. *Environmental Research Letters*, 10(9), 095009,
728 2015.

729 Zimov, S. A., Schuur, E. A., & Chapin III, F. S.: Permafrost and the global carbon
730 budget. *Science(Washington)*, 312(5780), 1612-1613, 2006.

731 Zoltai, S. C.: Permafrost distribution in peatlands of west-central Canada during the Holocene
732 warm period 6000 years BP. *Géographie physique et Quaternaire*, 49(1), 45-54, 1995.

733

734

735

736

737

738

739

740

741 Table 1. Description of sites and variables used for parameterizing the core carbon and nitrogen
 742 module (CNDM).

Site ^a	Vegetation	Observed variables for CNDM parameterization	References
APEXCON	Moderate rich open fen with sedges (<i>Carex</i> sp.), spiked rushes (<i>Eleocharis</i> sp.), <i>Sphagnum</i> spp., and brown mosses (e.g., <i>Drepanocladus aduncus</i>)	Mean annual aboveground NPP in 2009; Mean annual belowground NPP in 2009; Aboveground biomass in 2009	Chivers et al. (2009) Turetsky et al. (2008) Kane et al. (2010) Churchill et al. (2011)
APEXPER	Peat plateau bog with black spruce (<i>Picea mariana</i>), <i>Sphagnum</i> spp., and feather mosses		

743
 744 ^aThe Alaskan Peatland Experiment (APEX) site is adjacent to the Bonanza Creek Experimental Forest (BCEF) site,
 745 approximately 35 km southwest of Fairbanks, AK. The area is classified as continental boreal climate with a mean annual
 746 temperature of -2.9°C and annual precipitation of 269 mm, of which 30% is snow (Hinzman et al., 2006).

747

748

749 Table 2. Carbon pools and fluxes used for calibration of CMDM.

Annual Carbon Fluxes or Pools ^a	<i>Sphagnum</i> Open Fen		<i>Sphagnum</i> -Black Spruce Bog		References
	Observation	Simulation	Observation	Simulation	
NPP	445±260	410	433±107	390	Turetsky et al. (2008), Churchill (2011)
Aboveground Vegetation Carbon	149-287		423		Saarinen et al. (1996)
Belowground Vegetation Carbon	347-669		987		Moore et al. (2002)
Total Vegetation Carbon Density	496-856	800	1410	1300	Zhuang et al. (2002)
Litter Fall Carbon Flux	300	333	300	290	Tarnocai et al. (2009)
Methane Emission Flux	19.5	19.2	9.7	12.8	Kuhry and Vitt (1996)

750
 751 ^a Units for annual net primary production (NPP) and litter fall carbon are g C m⁻² yr⁻¹. Units for vegetation carbon density are
 752 g C m⁻². Units for Methane emissions are g C – CH₄ m⁻² yr⁻¹. The simulated total annual methane fluxes were compared with
 753 the observations at APEXCON in 2005 and SPRUCE in 2012. A ratio of 0.47 was used to convert vegetation biomass to carbon
 754 (Raich 1991).

755

756

757

758

759

760

761

762

763

764 Table 3. Assignment of biomized fossil pollen data to the vegetation types in TEM (He et al.,
 765 2014).

TEM upland vegetation	TEM peatland vegetation	BIOMISE code
Alpine tundra		CUSH DRYT PROS
Moist tundra	<i>Sphagnum</i> spp. open fen	DWAR SHRU
Boreal evergreen needleleaf and mixed forest		TAIG COCO CLMX
Boreal deciduous broadleaf forest	<i>Sphagnum</i> -black spruce bog	COMX
		CLDE

766

767

768 Table 4. Relations between peatland basal age and vegetation distribution.

Peatland basal age	Vegetation types	Location in Alaska
15-11 ka	alpine tundra	south, northwestern, and southeastern coast
11-10 ka	moist tundra boreal evergreen needleleaf forest boreal deciduous broadleaf forest	south, north, and southeastern coast
10-9 ka	moist tundra boreal evergreen needleleaf forest boreal deciduous broadleaf forest	east central part south and north coast central part
9-5 ka	moist tundra boreal evergreen needleleaf forest	central part
5 ka-1900 AD	moist tundra boreal evergreen needleleaf forest	west coast

769

770

771

772

773

774

775

776

777

778

779

780 Table 5. Sites used for comparison of carbon accumulation rates between simulation and
 781 observation (Jones and Yu, 2010).

Site name	Location	Peatland type	Latitude	Longitude	Dating method	No. of dates	Basal age (cal yr BP)	Time-weighted Holocene accumulation rates (g C m ⁻² yr ⁻¹)
Kenai Gasfield	Alaska, USA	fen	60°27'N	151°14'W	AMS	12	11,408	13.1
No Name Creek	Alaska, USA	fen	60°38'N	151°04'W	AMS	11	11,526	12.3
Horsetrail fen	Alaska, USA	rich fen	60°25'N	150°54'W	AMS	10	13,614	10.7
Swanson fen	Alaska, USA	poor fen	60°47'N	150°49'W	AMS	9	14,225	5.7

782

783

784

785

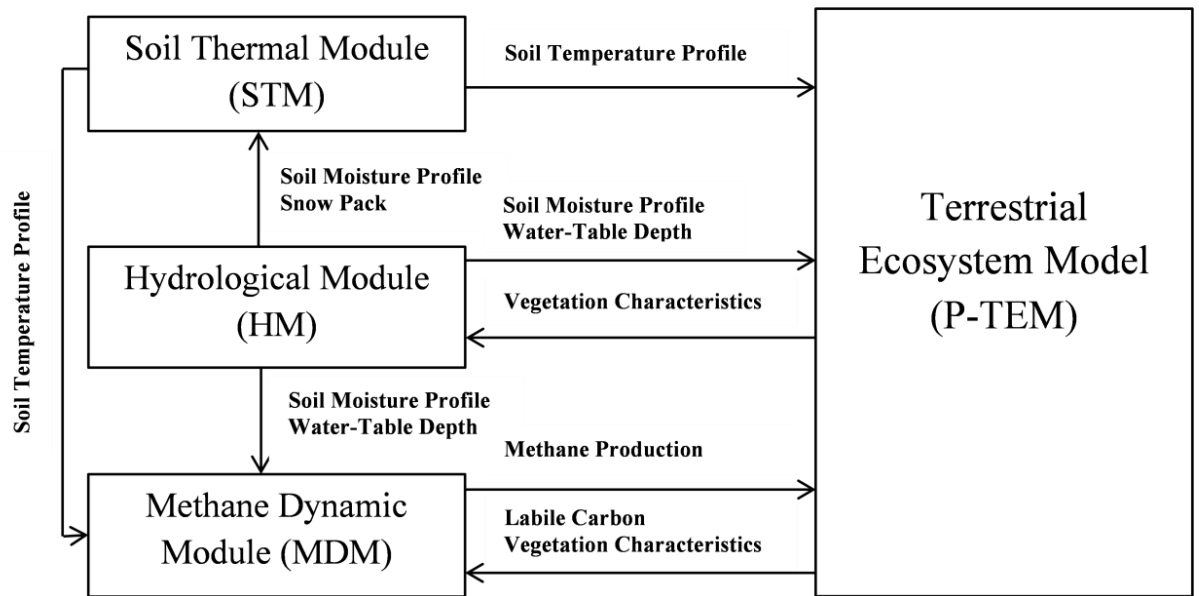
786

787

788

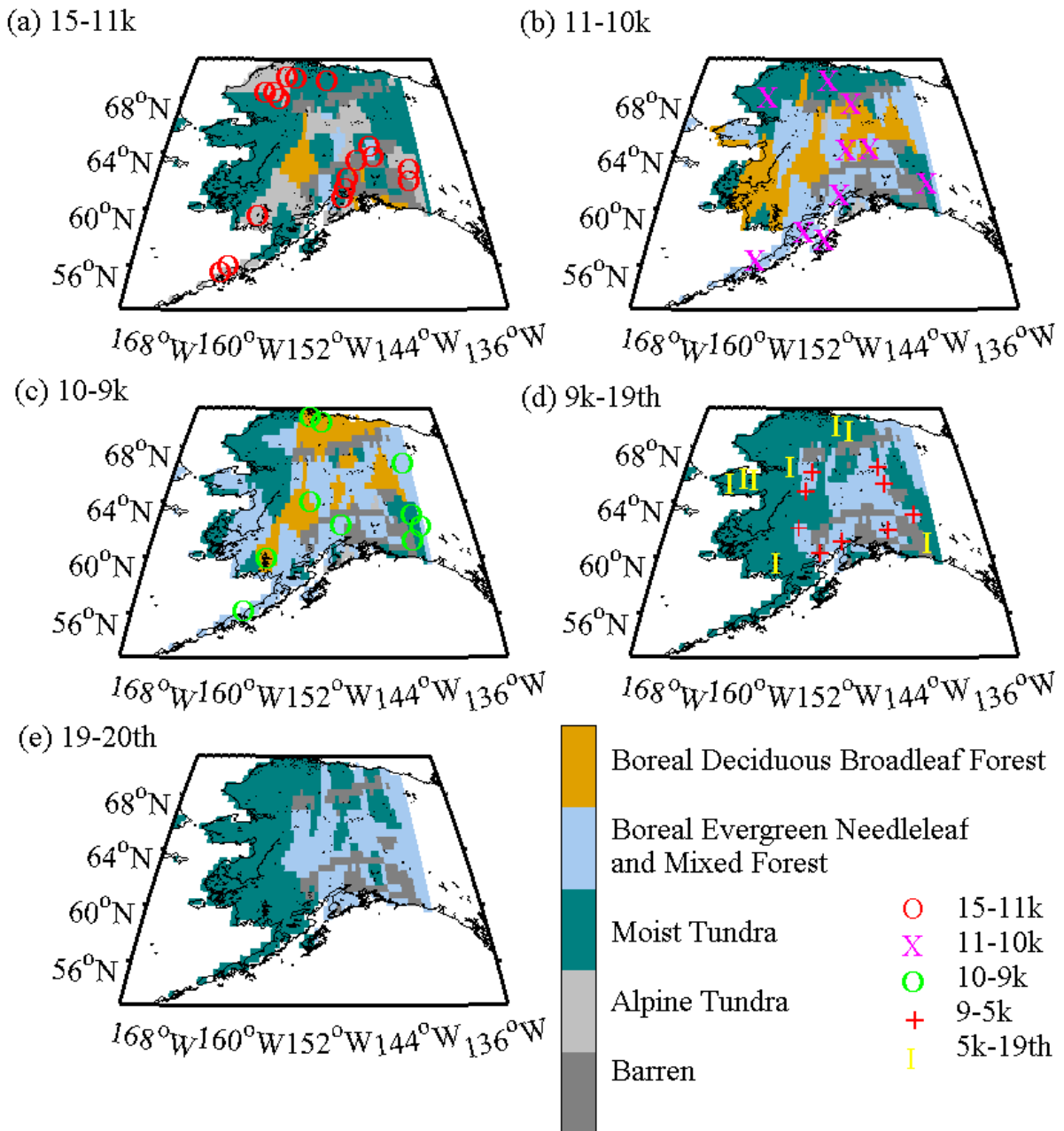
789

790



791
 792 Figure 1. P-TEM (Peatland-Terrestrial Ecosystem Model) framework includes a soil thermal
 793 module (STM), a hydrologic module (HM), a carbon/ nitrogen dynamic model (CNDM), and a
 794 methane dynamics module (MDM) (Wang et al., 2016).

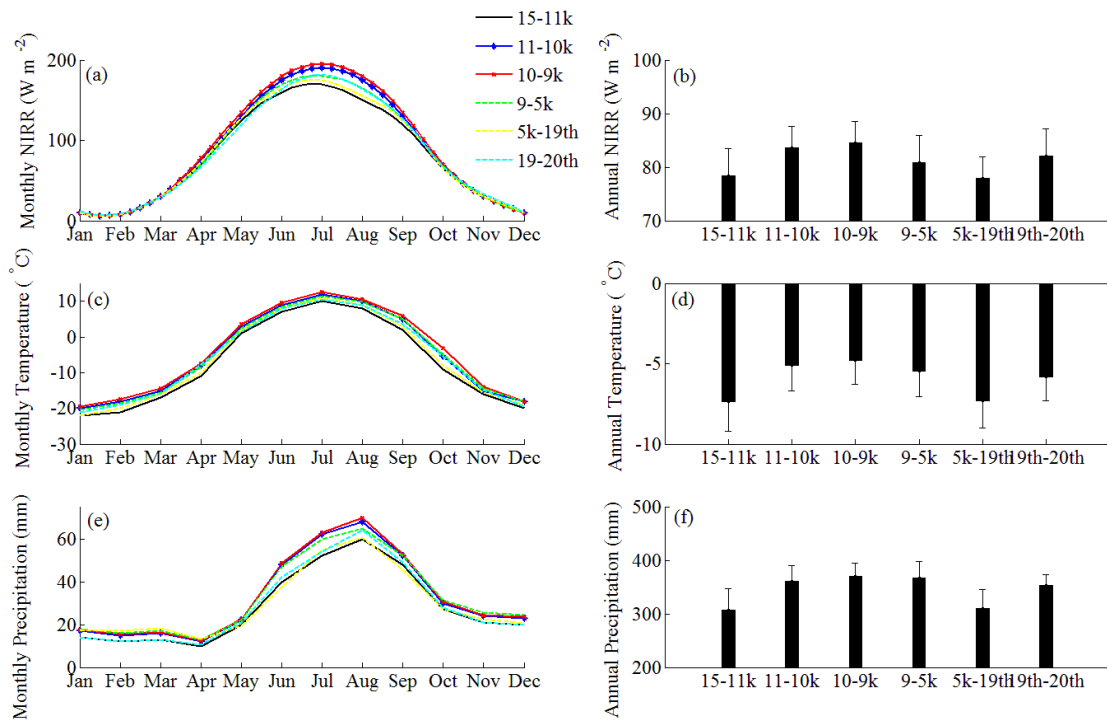
795
 796
 797
 798
 799
 800
 801
 802
 803
 804
 805
 806
 807
 808



809
 810 Figure 2. Alaskan vegetation distribution maps reconstructed from fossil pollen data during (a)
 811 15-11 ka, (b) 11-10 ka, (c) 10-9 ka, (d) 9 ka -1900 AD, and (e) 1900-2000 AD (He et al., 2014).
 812 Symbols represent the basal age of peat samples (n = 102) in Gorham et al. (2012). Each
 813 symbol indicates 1-3 peat samples in the map. Peat samples with basal age 9-5k and 5k-19th are
 814 shown in map (d) as there is no change of vegetation distribution during 9k-19th. Barren refers to
 815 mountain range and large water body areas that can not be interpolated.

816

817



819
 820 Figure 3. Simulated Paleo-climate and other input data from 15 ka to 2000 AD: (a) mean
 821 monthly and (b) mean annual net incoming solar radiation (NIRR, $W m^{-2}$), (c) mean monthly
 822 and (d) mean annual air temperature ($^{\circ}C$), (e) mean monthly, and (f) mean annual precipitation
 823 (mm) (Timm and Timmermann, 2007; He et al., 2014).

824

825

826

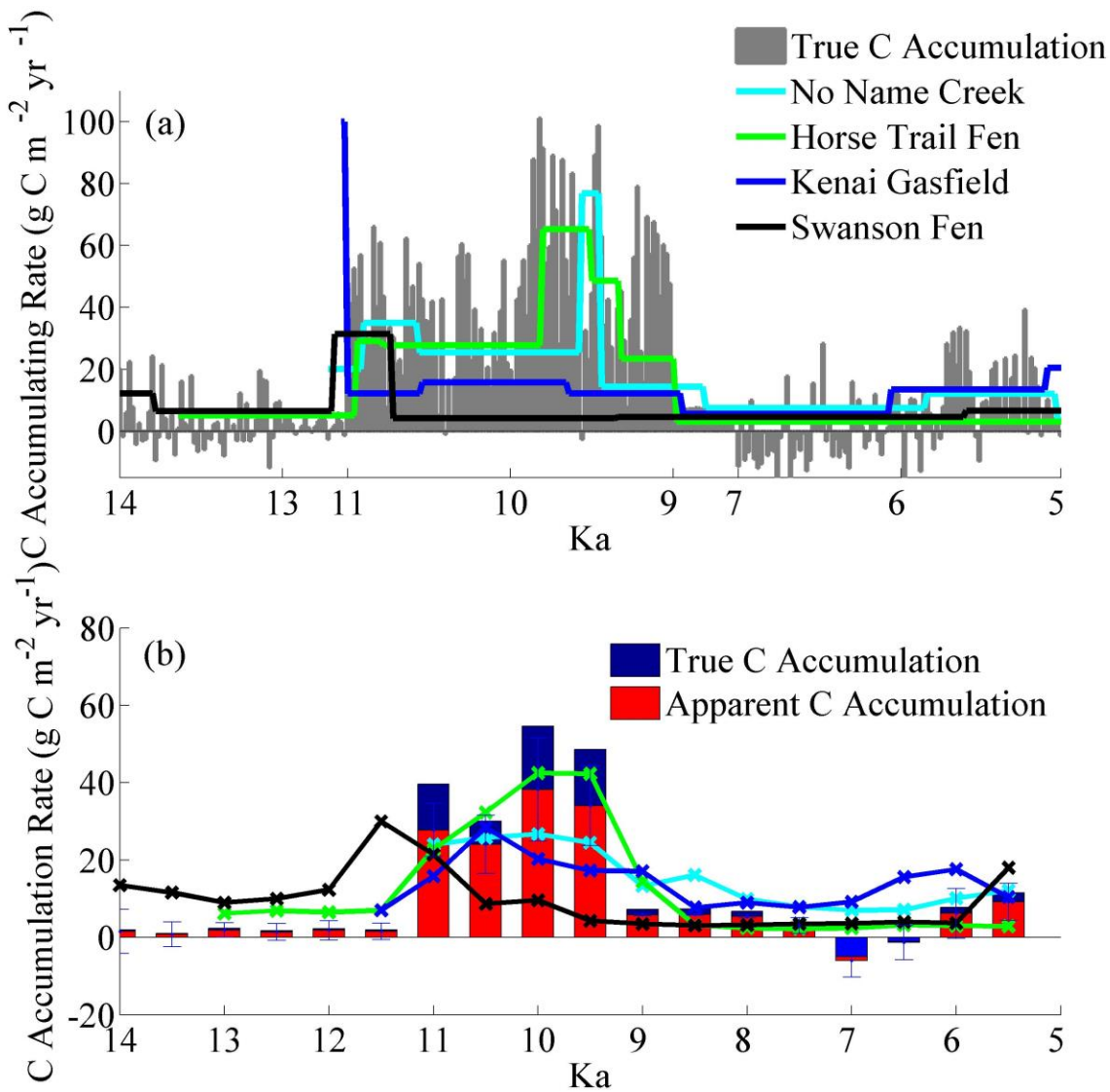
827

828

829

830

831



832 Figure 4. Simulated and observed carbon accumulation rates from 15 ka to 5 ka in 20-yr bins (a)
833 and 500-yr bins with standard deviation (b) for No Name Creek, Horse Trail Fen, Kenai Gasfield,
834 and Swanson Fen. Peat-core data were from Jones and Yu (2010).
835

836

837

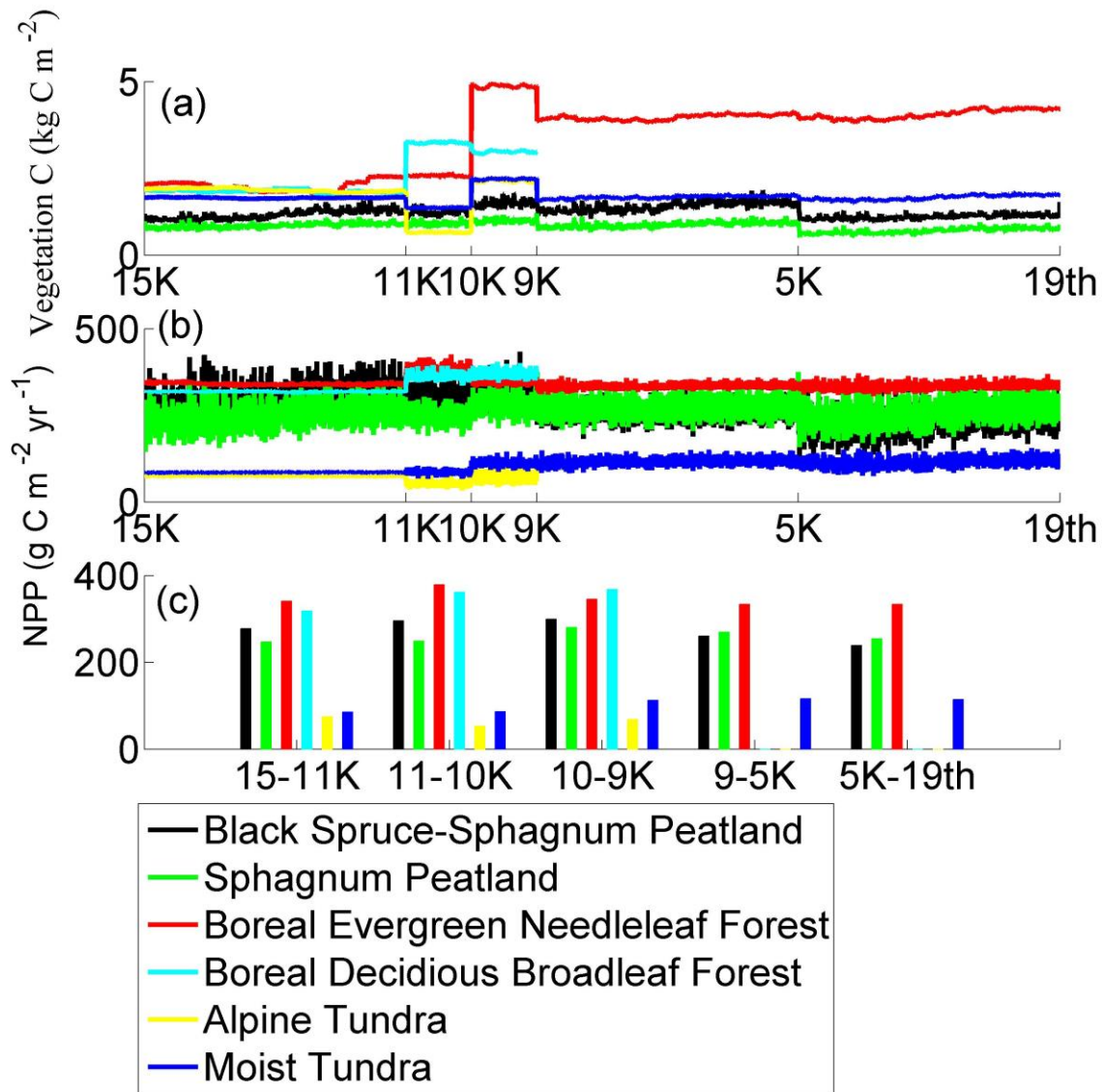
838

839

840

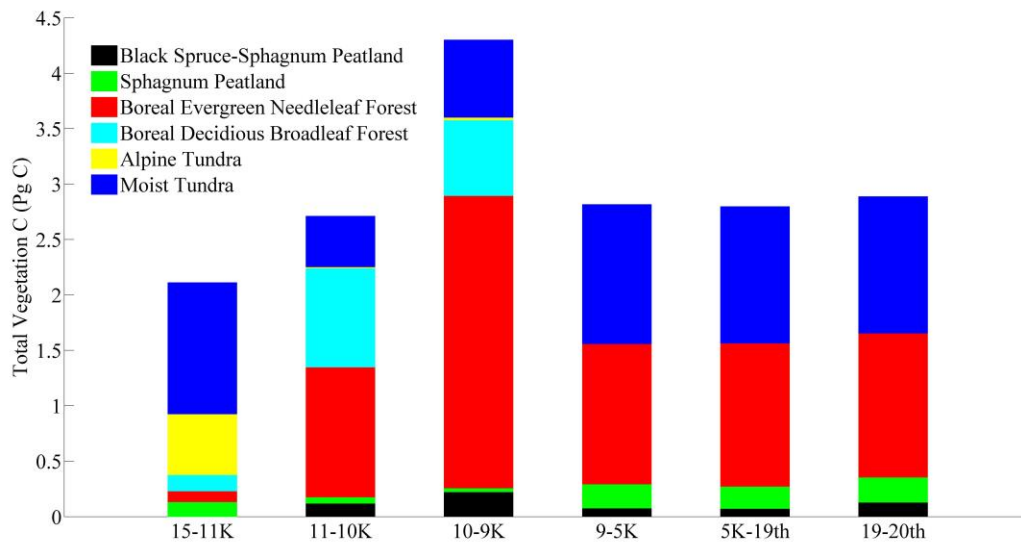
841

842
843
844



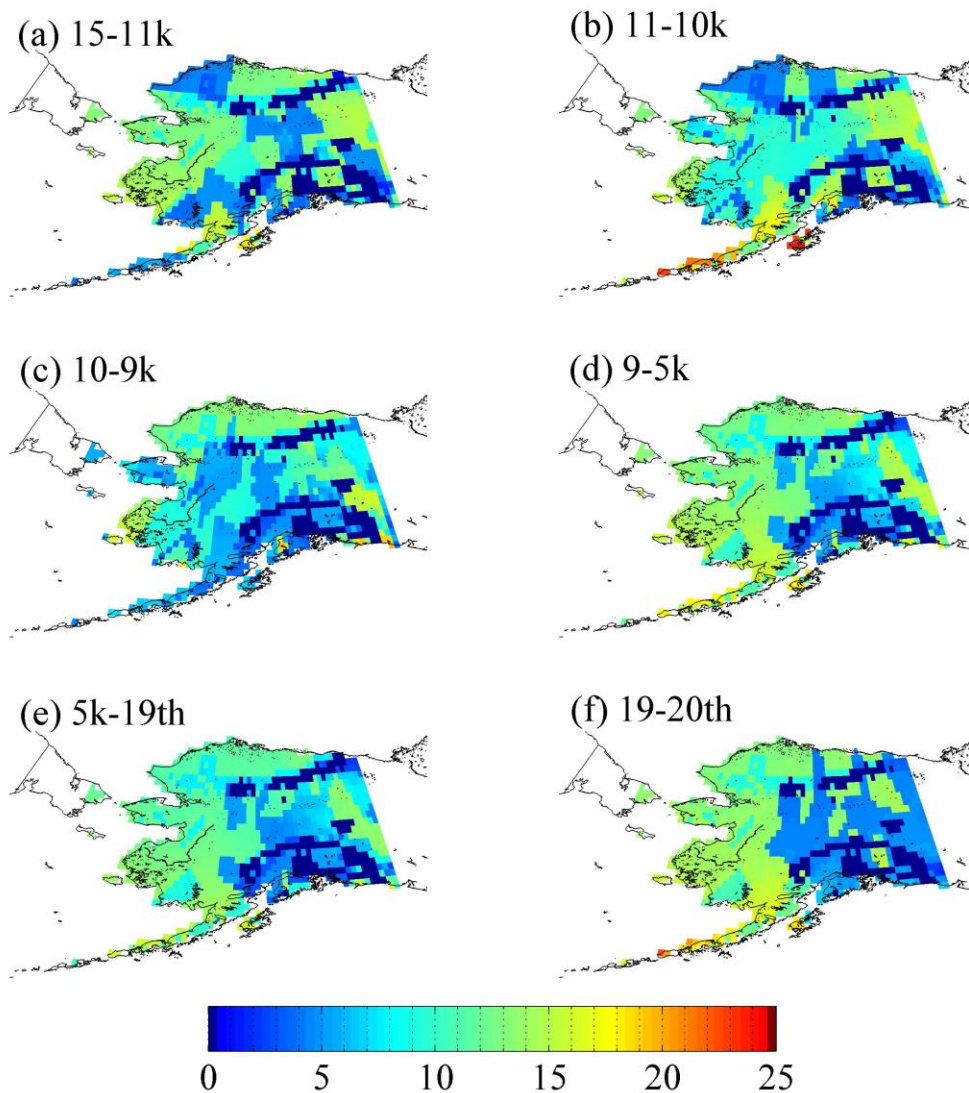
845
846 Figure 5. Simulated (a) mean vegetation carbon density (kg C m^{-2}) of different vegetation types,
847 (b) annual NPP ($\text{g C m}^{-2} \text{yr}^{-1}$), and (c) long-term NPP ($\text{g C m}^{-2} \text{yr}^{-1}$).

848
849
850



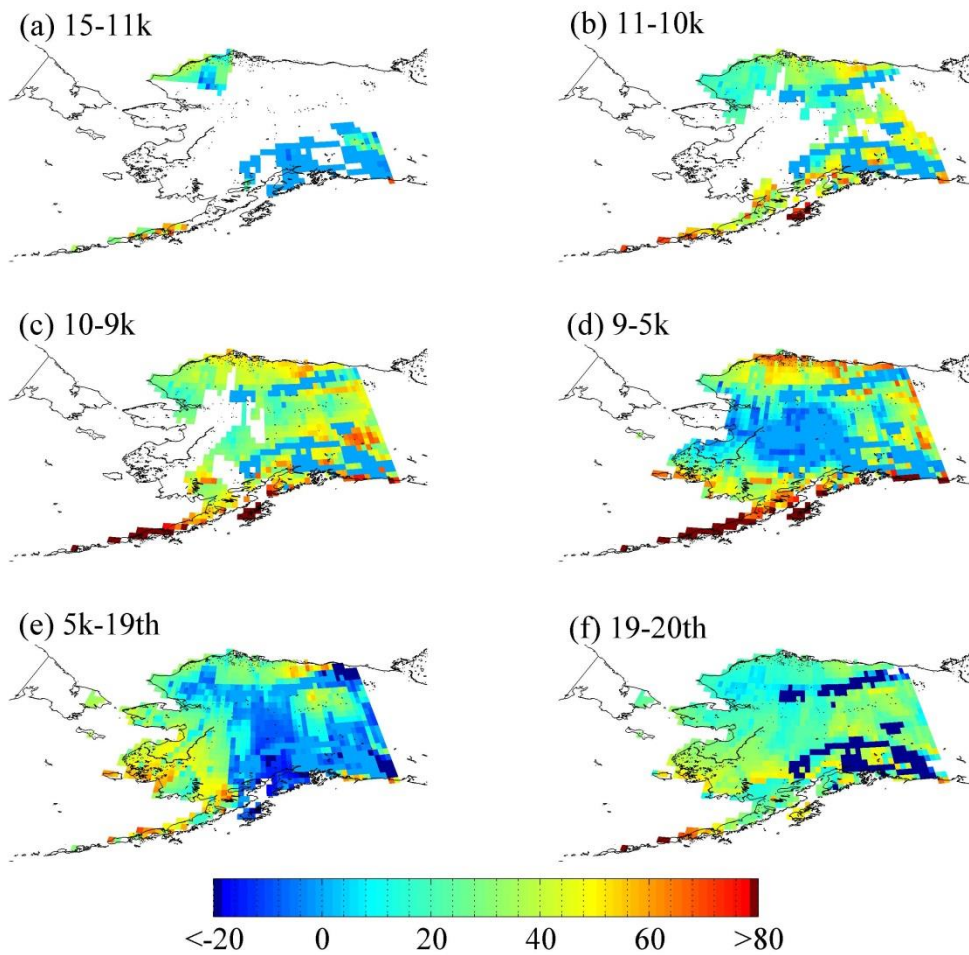
851
 852 Figure 6. Total C (Pg C) stored in Alaskan vegetation for different time periods.

853



854
 855 Figure 7. Average non-peatland (mineral) SOC density (kg C m^{-2}) during (a) 15-11 ka, (b) 11-
 856 10 ka, (c) 10-9 ka, (d) 9-5 ka, (e) 5 ka -1900 AD, and (f) 1900-2000 AD. The period of 9k-19th in
 857 Figure 2d is separated into 9-5k and 5k-19th.

858



859
 860 Figure 8. Peatland area expansion and peat soil C accumulation per 1000 years ($\text{kg C m}^{-2} \text{ kyr}^{-1}$)
 861 during (a) 15-11 ka, (b) 11-10 ka, (c) 10-9 ka, (d) 9-5 ka, (e) 5 ka -1900 AD, and (f) 1900-2000
 862 AD. The amount of C represents the C accumulation as the difference between the peat C
 863 amount in the final year and the first year in each time slice. The period of 9k-19th in Figure 2d is
 864 separated into 9-5k and 5k-19th.

865

866

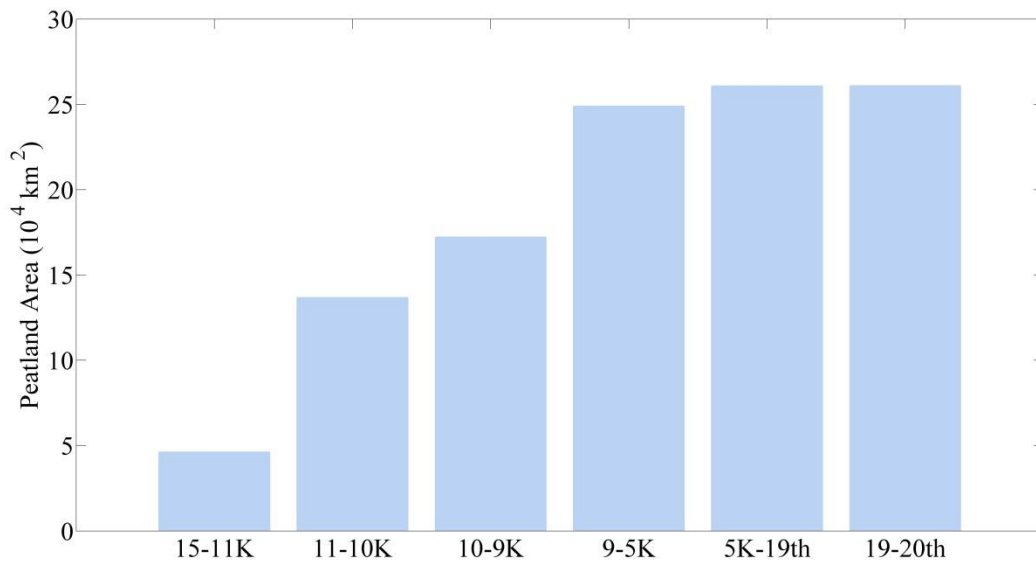
867

868

869

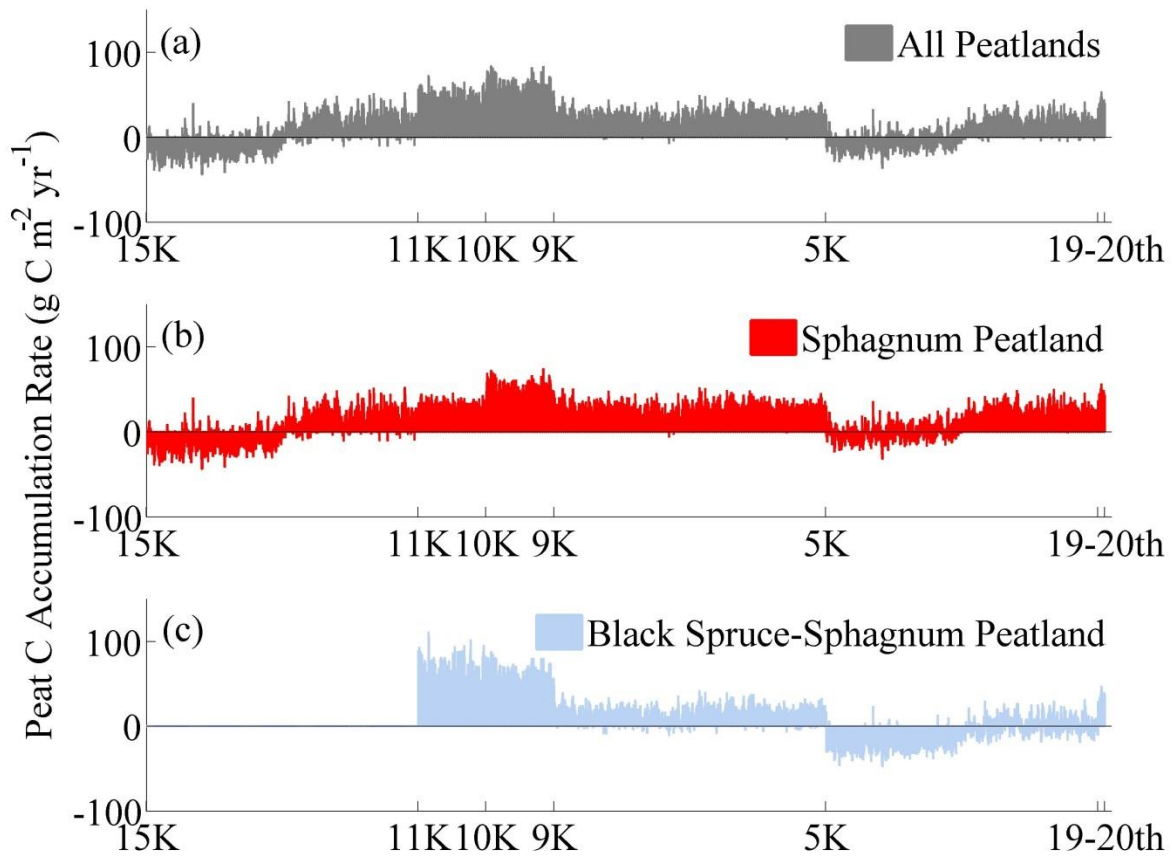
870

871



872
873 Figure 9. Peatland expansion area (10^4 km^2) in different time slices.

874

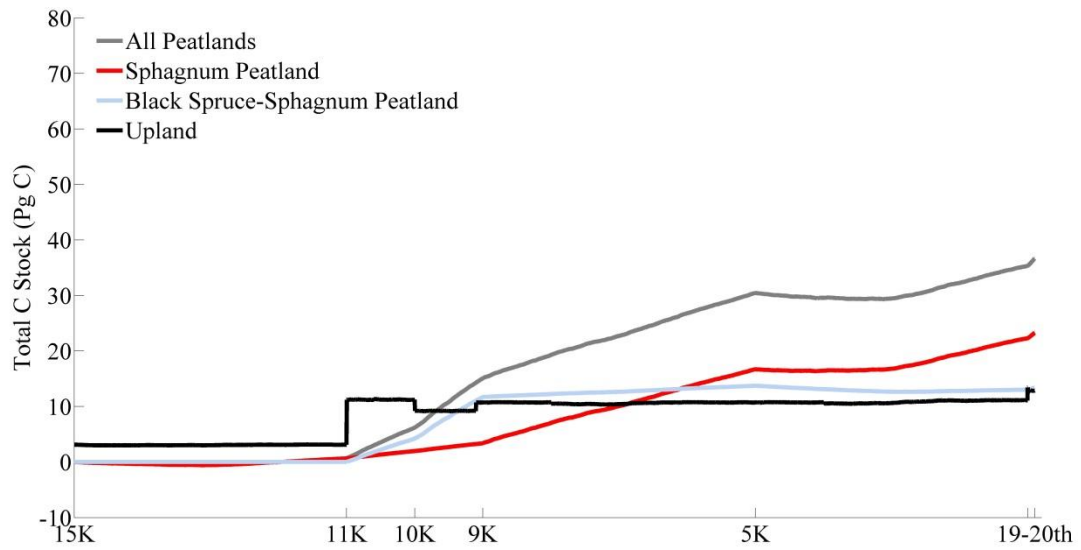


875

876 Figure 10. Bars of peatland mean C accumulation rates from 15 ka to 2000 AD for (a) weighted
 877 average of all peatlands, (b) *Sphagnum* open peatlands, and (c) *Sphagnum*-black spruce peatlands.

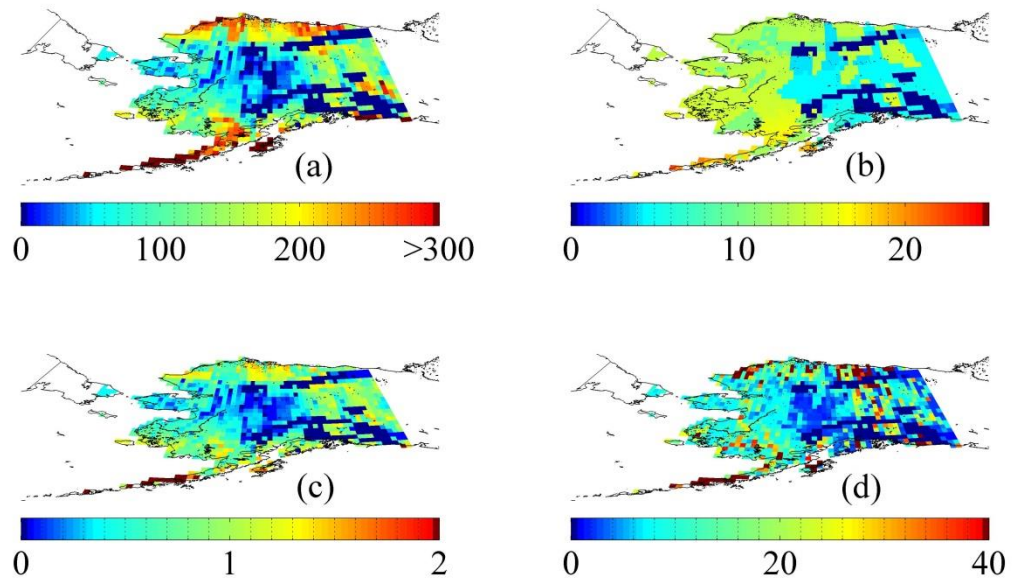
878

879

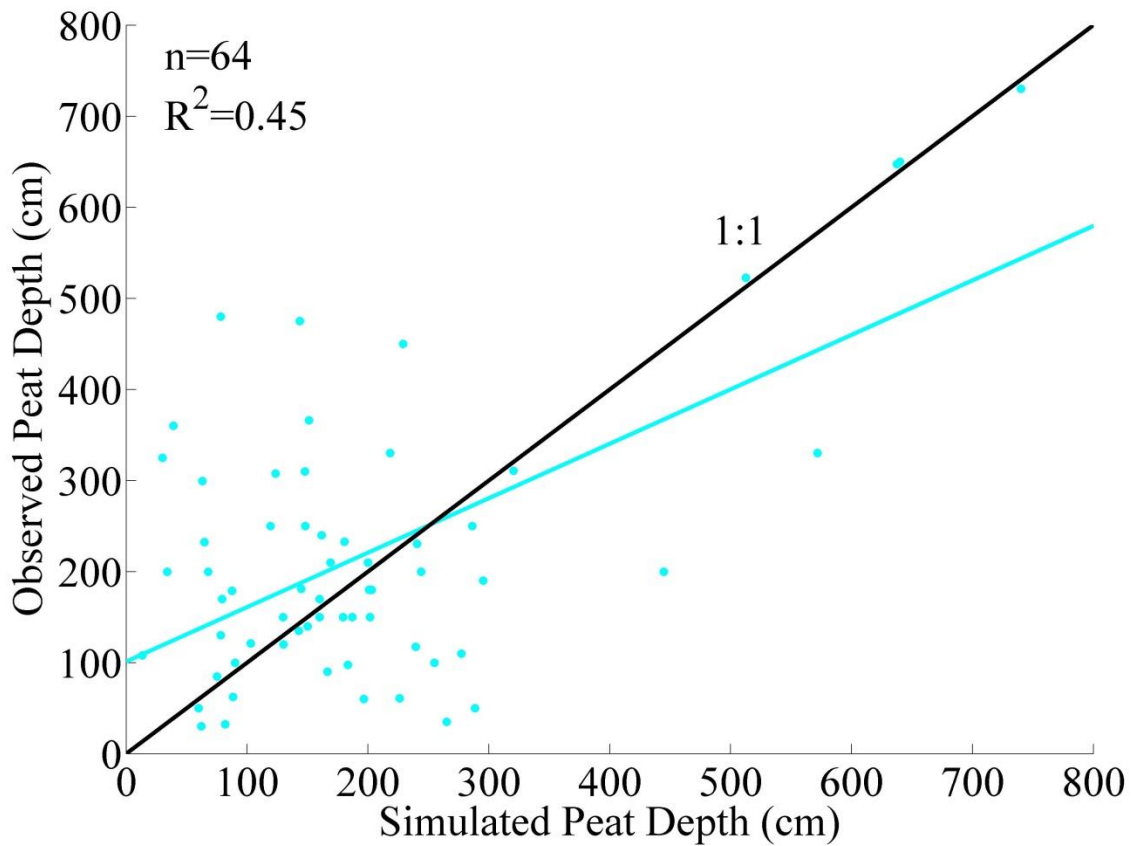


880
 881 Figure 11. Total C stock accumulated from 15 ka to 2000 AD for all peatlands, *Sphagnum* open
 882 peatlands, *Sphagnum*-black spruce peatlands, and upland soils.

883
 884
 885
 886
 887
 888
 889
 890
 891
 892

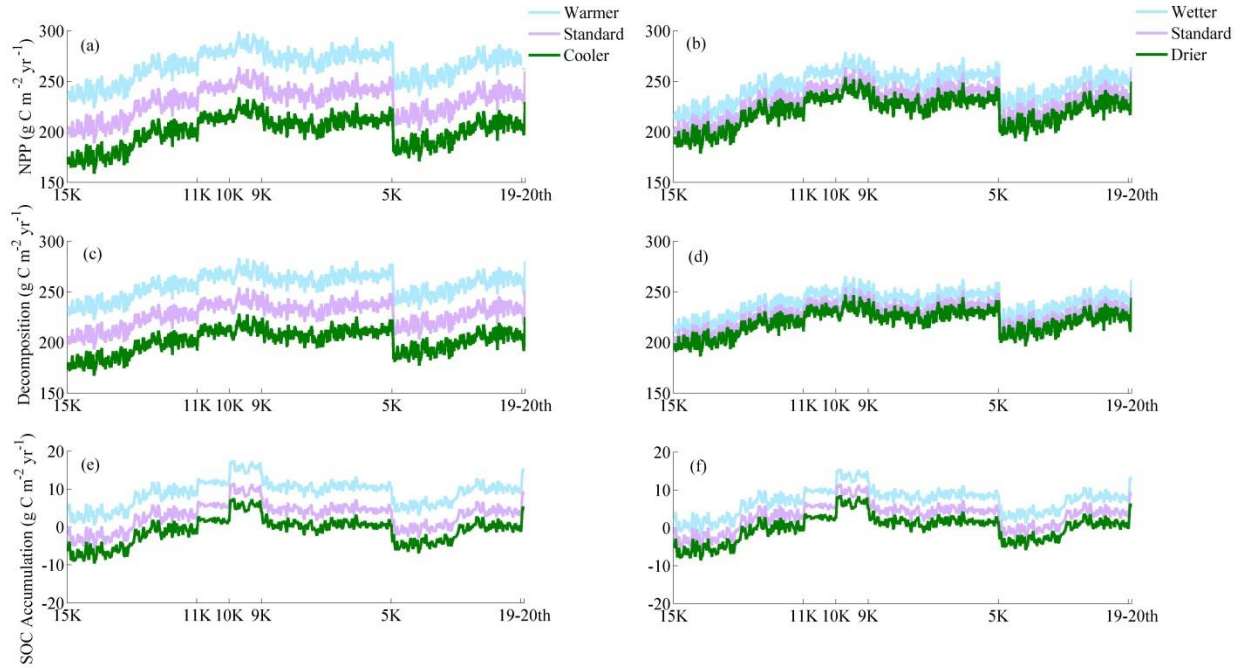


893
 894 Figure 12. Spatial distribution of (a) total peat SOC density (kg C m^{-2}), (b) total mineral SOC
 895 density (kg C m^{-2}), (c) total peat depth (m), and (d) area-weighted total (peatlands plus non-
 896 peatlands) SOC density (kg C m^{-2}) in Alaska from 15 ka to 2000 AD.



897
 898 Figure 13. Field-based estimates and model simulations for peat depths in Alaska: The observed
 899 and simulated data are extracted from the same grids on the map. Linear regression line (cyan) is
 900 compared with the 1:1 line. The linear regression is significant ($P < 0.001$, $n = 64$) with $R^2 = 0.45$,
 901 slope = 0.65, and intercept = 101.05 cm. The observations of >1000 cm are treated as outliers.

902
 903
 904
 905



906

907 Figure 14. Temperature and precipitation effects on (a)(b) annual NPP, (c)(d) annual SOC
 908 decomposition rate (aerobic plus anaerobic), and (e)(f) annual SOC accumulation rate of Alaska.
 909 A 10-year moving average was applied.

910

911

912

913

914

915

916